Suppressors of mRNA Decapping Defects Restore Growth Without Major Effects on mRNA Decay Rates or Abundance

Minseon Kim and Ambro van Hoof[1]
Microbiology and Molecular Genetics Department, University of Texas Health Science Center at Houston, Houston, Texas 77030
ORCID IDs: 0000-0001-5299-0008 (M.K.); 0000-0002-7800-9764 (A.v.H.)

ABSTRACT Faithful degradation of mRNAs is a critical step in gene expression, and eukaryotes share a major conserved mRNA decay pathway. In this major pathway, the two rate-determining steps in mRNA degradation are the initial gradual removal of the poly(A) tail, followed by removal of the cap structure. Removal of the cap structure is carried out by the decapping enzyme, containing the Dcp2 catalytic subunit. Although the mechanism and regulation of mRNA decay is well understood, the consequences of defects in mRNA degradation are less clear. Dcp2 has been reported as either essential or nonessential. Here, we clarify that Dcp2 is not absolutely required for spore germination and extremely slow growth, but in practical terms it is impossible to continuously culture *dcp2Δ* under laboratory conditions without suppressors arising. We show that null mutations in at least three different genes are each sufficient to restore growth to a *dcp2Δ*, of which *kap123Δ* and *tl(gag)gΔ* appear the most specific. We show that *kap123Δ* and *tl(gag)gΔ* suppress *dcp2* by mechanisms that are different from each other and from previously isolated *dcp2* suppressors. The suppression mechanism for *tL(GAG)G* is determined by the unique GAG anticodon of this tRNA, and thus likely by translation of some CUC or CUU codons. Unlike previously reported suppressors of decapping defects, these suppressors do not detectably restore decapping or mRNA decay to normal rates, but instead allow survival while only modestly affecting RNA homeostasis. These results provide important new insight into the importance of decapping, resolve previously conflicting publications about the essentiality of *DCP2*, provide the first phenotype for a *tl(gag)g* mutant, and show that multiple distinct mechanisms can bypass Dcp2 requirement.

KEYWORDS *DCP2*; mRNA decay; decapping; *KAP123*; *tL(GAG)G*

EUKARYOTES share two major messenger RNA (mRNA) decay pathways that are both carried out by exonucleolytic digestion. mRNA degradation is initiated by gradual shortening of the poly(A) tail, followed by Xrn1-mediated 5′ to 3′ decay and RNA exosome-mediated 3′ to 5′ decay (Parker 2012). Because Xrn1 can only degrade RNAs with a 5′-monophosphate (Stevens and Poole 1995; Jinek *et al.* 2011), removal of the 5′ cap structure by Dcp2 is required in the 5′ to 3′ decay pathway. Importantly, deleting either *DCP2* or *XRN1* results in stabilization of many yeast mRNAs (Larimer *et al.* 1992; Dunckley and Parker 1999; He *et al.* 2003). The stabilization of mRNAs in *dcp2* mutants indicates that yeast Dcp2 is the major decapping enzyme, and the 5′ to 3′ pathway is the major mRNA decay pathway. Other enzymes capable of decapping mRNAs have been described both in yeast and other organisms (Jiao *et al.* 2010; Song *et al.* 2010; Li *et al.* 2011; Fujimura and Esteban 2012; Zhou *et al.* 2015; Grudzien-Nogalska *et al.* 2016; Doamekpor *et al.* 2020), but their role in bulk cytoplasmic mRNA degradation has not been fully defined. Consistent with its importance for mRNA decay, deletion of *XRN1* causes a slow growth defect, while the phenotype of *dcp2Δ* is reported inconsistently among different studies. Some studies have reported that *dcp2Δ* is viable but slow-growing, while others reported that *dcp2Δ* is lethal (Dunckley and Parker 1999; Giaever *et al.* 2002; Geisler *et al.* 2012; He and Jacobson

doi: https://doi.org/10.1534/genetics.120.303641
Manuscript received August 25, 2020; accepted for publication September 28, 2020; published Early Online September 30, 2020.
Supplemental material available at figshare: https://doi.org/10.6084/m9.figshare.12985820.
[1]Corresponding author: Microbiology and Molecular Genetics Department, University of Texas Health Science Center at Houston, 6431 fannin, msb 1.212, Houston, TX 77030. E-mail: ambro.van.hoof@uth.tmc.edu

2015). It has been speculated that this difference between studies is attributable to differences between the strains used (He and Jacobson 2015), but this has not been critically analyzed.

Previously, suppressor screens of budding yeast decapping mutants (*dcp1* or *dcp2* conditional mutants) have identified *EDC1*, *EDC2*, *EDC3*, *SBP1*, and *DCP2* itself as high-copy suppressors (Dunckley and Parker 1999; Dunckley *et al.* 2001; Kshirsagar and Parker 2004; Segal *et al.* 2006). In each case, the improved growth caused by suppressors was correlated with improved decapping activity and mRNA degradation, suggesting that the essential function of the Dcp1-Dcp2 decapping enzyme is indeed mRNA decapping. Although these studies showed that the major function of Dcp1 and Dcp2 is mRNA decapping, they are limited to high-copy suppressor screens of conditional alleles in the decapping enzyme, which may not have revealed the full functions of Dcp2.

To further understand the function of Dcp2, we sought to identify suppressors of the growth defect of a decapping mutant by a complementary experimental evolution of a *dcp2* null strain, which can be more powerful in identifying smaller effects and double mutants. Surprisingly, we identified genes that have no obvious connection to mRNA degradation. Among the genes we identified, we focused on the karyopherin *KAP123* and the leucine tRNA *tL(GAG)G* that are recurrently mutated. We showed that a null mutation of each gene is sufficient to suppress the growth phenotype of *dcp2Δ*, and that *kap123Δ* and *tl(gag)gΔ* have additive effects. We also show that previously reported viable *dcp1Δ* and *dcp2Δ* strains had undetected mutations in *KAP123*, suggesting that they were mistakenly reported as viable due to the suppressor mutations. Instead, our results suggest that *dcp2Δ* grows extremely slowly and cannot be continuously cultured under standard conditions. Interestingly, suppression of the growth defect of *dcp2Δ* is not caused by improved cytoplasmic mRNA decay. Absence of Dcp2 causes a global disturbance of the transcriptome including not only mRNA, but also noncoding RNA, and the suppressor mutations we identified do not restore the transcriptome to normal. However, we do detect a widespread but modest amplitude effect in partially restoring RNA homeostasis. Whether these modest effects on transcripts are a cause or effect of improved growth, or a mixture of both, is not clear. These results indicate that the extremely poor growth of a strain lacking the decapping enzyme can be overcome by several independent mechanisms that have modest effects on the transcriptome compared to the global disruption of the transcriptome caused by *dcp2* mutations.

Materials and Methods

Strains, plasmids, and oligonucleotides

The *DCP2/dcp2Δ* heterozygous diploid in the BY4743 (S288C) background was obtained from Open Biosystems, Huntsville, AL and all other strains (Supplemental Material, Table S1) used are derived from it through standard genetic procedures. Plasmids were generated by standard procedures and are listed in Table S2. Oligonucleotides (Sigma-Aldrich, St. Louis, MO) used in this study are listed in Table S3.

Yeast growth conditions

Yeast was grown either in standard yeast extract peptone (YEP) media containing 2% dextrose or galactose or in synthetic complete media lacking amino acids (Sunrise Science) as required. G418 (0.67 mg/ml), hygromycin B (325 U/ml), or clonNAT (100 μg/ml) was added to YEP plus dextrose media to select for knockouts. Cells were incubated at 30° unless otherwise indicated. The *dcp2-7* cultures were incubated for 60 or 90 min at 37° to inactivate the decapping enzyme for the *GAL* mRNA stability and transcriptome sequencing experiments, respectively.

To induce sporulation, diploid cells were grown in nutrient-depleted media for 4–5 days. Sporulated cells were resuspended in water with Glusulase (Perkin Elmer). This reaction was incubated at 30° for 30 min. Ascus digestion was terminated using water. Haploids were obtained either by tetrad dissection or by random spore isolation (Rockmill *et al.* 1991). The *dcp2Δ* spores from the starting haploid formed pinprick-size colonies after 2 weeks of incubation at room temperature.

Experimental evolution was initiated from four haploid *dcp2Δ* strains, each derived from a different tetrad. Duplicate 5 ml cultures of each of the four haploid *dcp2Δ* strains were inoculated in YEP containing 2% dextrose, G418 (167 mg/liter), and ampicillin (50 mg/liter). Cultures were grown at 30° until the OD_{600} of the culture reached > 8.5. Then, 10 μl of this culture (containing on the order of 10^6 yeast cells) were transferred into 5 ml of fresh media of the same type. This culturing and 500-fold dilution was repeated 30 times. A 500-fold (or $2^{8.97}$) dilution represents ~9 doublings. Thus, after 30 cycles of culture and dilution the cultures had gone through ~270 generations.

For the growth assay on solid media, exponentially growing cells were serially diluted (fivefold) and spotted on the indicated media. For the growth assay in liquid media, exponentially growing cells were diluted to OD_{600} of 0.1, and transferred to a 96-well plate. Cells were incubated at 30° in a BioTek's Synergy Mx Microplate Reader. OD_{600} was measured every 10 min for ~15 hr. Collected data were processed through Gen5 (BioTek).

Microscopy

To examine cell morphology, exponentially growing cells were analyzed on an Olympus BX60 microscope.

Whole-genome sequencing analysis

Total genomic DNA was isolated from exponentially growing cells using a phenol-chloroform extraction method and further purified with the use of a DNeasy Blood & Tissue Kit (QIAGEN, Valencia, CA) and a MasterPure Yeast DNA

Purification Kit (Lucigen). PE150 libraries of the evolved strains were prepared and sequenced by Novogen.

To identify mutations, sequencing reads were trimmed with Trim Sequences (http://hannonlab.cshl.edu/fastx_toolkit/), quality checked with FastQC (http://www.bioinformatics.babraham.ac.uk/projects/fastqc/), and mapped with Bowtie2 (Langmead *et al.* 2009) to *Saccharomyces cerevisiae* reference genome R64-1-1 (www.ensembl.org). The overall alignment rate was ~91–99%. Before calling variants, BAM data sets for the individual *dcp2Δ* strain and heterozygous diploid *DCP2/dcp2Δ* strain were merged using MergeSamFiles (http://broadinstitute.github.io/picard/). Data sets were further processed for left realignment through BamLeftAlign (https://arxiv.org/abs/1207.3907). To call all the variants, we used FreeBayes (https://arxiv.org/abs/1207.3907) for detection and SnpEff 4.3 (Cingolani *et al.* 2012) for annotation. Integrated Genome Viewer (https://software.broadinstitute.org/software/igv/download) was used to inspect candidate SNPs. True mutations were differentiated from sequencing errors and preexisting SNPs by being supported by the consensus of the reads in the evolved isolate(s), but not by the reads from the other evolved isolates or the heterozygous diploid *DCP2/dcp2Δ* strain that we had previously sequenced. The vast majority of preexisting SNPs that we identified in the *DCP2/dcp2Δ* starting diploid have previously been described in the genome sequences of BY4741 (http://sgd-archive.yeastgenome.org/sequence/strains/BY4741/) and/or BY4742 (http://sgd-archive.yeastgenome.org/sequence/strains/BY4742/). BY4741 and BY4742 are the parents of the diploid BY4743 strain, which in turn is the parent of our *DCP2/dcp2Δ* starting diploid.

MiModD Deletion Calling (https://sourceforge.net/projects/mimodd/) was used to search for deletions, which identified the *ura3Δ*, *his3Δ*, *met15Δ*, *lys2Δ*, and *leu2Δ* deletions of BY4743, but no other deletions. MiModD Coverage Statistics (https://sourceforge.net/projects/mimodd/) was used to measure coverage depth by chromosome, to search for aneuploidy.

Protein analysis

Total protein was extracted in IP50 buffer [50 mM Tris-HCl (pH 7.5), 50 mM NaCl, 2 mM $MgCl_2$, 0.1% Triton X-100] with 0.007% β-mercaptoethanol and 0.00174% PMSF, and complete protease EDTA-free mini tablet (Roche) by bead beating and analyzed by Western blot. Blots were probed with anti-Kap123 at 1:5000 (Patel and Rexach 2008; Floch *et al.* 2015) and anti-Pgk1 at 1:10,000 (Invitrogen, Carlsbad, CA), and developed using Amersham ECL Prime (GE Healthcare). Images were acquired and analyzed using an ImageQuant LAS 4000 biomolecular imager (GE Healthcare) and ImageQuant TL image analysis software.

RNA analysis using Northern blotting

For analyzing the steady-state RNA level, cells exponentially growing at 30° were harvested. For analyzing RNA stability, *dcp2-7* mutants were grown in YEP containing 2% galactose at 21° and transferred into a 37° incubator for 1 hr to inactivate the decapping enzyme. Cells were washed with YEP, and dextrose (40% stock solution) was added to a final concentration of 2% to repress transcription of the *GAL* genes. Although cells were incubated at 37°, samples were collected at the indicated time points and immediately frozen.

For RNA preparation, the harvested cell pellet was lysed by vortexing with glass beads. RNA was purified through two rounds of phenol/chloroform/LET (LiCl-EDTA-Tris HCl, pH8.0) and one additional chloroform extraction, and ethanol precipitated.

Total RNA was analyzed through Northern blotting. Briefly, 10 μg of total RNA was analyzed by electrophoresis on denaturing gels, either 1.3% agarose/formaldehyde gels for mRNA analysis or 6% polyacrylamide (19:1) 8M urea gel for transfer RNA (tRNA) analysis, as indicated. RNA was transferred to a nylon membrane and probed with ^{32}P 5′ end labeled oligonucleotides. For the Northern blots on mutant tRNAs, we prevented differences in detection efficiency by using probes that did not overlap with the mutations. Blots were imaged by phosphorimaging on a Typhoon FLA 7000 (GE Healthcare), and quantitated using ImageQuant software.

Transcriptome analysis

For RNA-sequencing (RNA-seq) analysis, cultures (biological triplicates) of exponentially growing cells were transferred into a 37° incubator and incubated for 90 min to inactivate the decapping enzyme before harvesting. Total RNA was extracted using the hot phenol method (He *et al.* 2008). For sequencing, poly(A)$^+$ selected RNA was used to construct a library for PE150 Illumina sequencing. Reads were submitted to Sequence Read Archive (SRA) under project number PRJNA626686. Raw reads were trimmed using Trim Galore! (http://www.bioinformatics.babraham.ac.uk/projects/trim_galore/), quality checked with FastQC (http://www.bioinformatics.babraham.ac.uk/projects/fastqc/), and mapped to reference genome R64-1-1 with TopHat2 (Kim *et al.* 2013). Gene expression level was determined with featureCounts (Liao *et al.* 2014) for genes identified in the annotation file from Ensembl (www.ensembl.org) and for XUTs (http://vm-gb.curie.fr/XUT/index.htm) (van Dijk *et al.* 2011). Differential gene expression was determined through DESeq2 (Love *et al.* 2014). Gene ontology (GO) analysis was performed through the GO Term Finder (version 0.86).

Finding kap123 mutations in published RNA-seq data

To determine whether previously published RNA-seq experiments inadvertently used *kap123* mutant strains and to identify the mutations, we downloaded raw RNA-seq reads from the European Bioinformatics Institute (https://www.ebi.ac.uk/ena). Reads were trimmed with Trim Galore!, quality checked with FastQC, and then aligned with TopHat2 to the R64-1-1 reference genome. Aligned reads were analyzed

in Integrated Genome Viewer. This identified the *kap123-Y687X* in three data sets from a *dcp2Δ* W303 strain (SRR4163304, SRR4163305, SRR4163306). For the *dcp1Δ* data sets (SRR4163301, SRR4163302), the TopHat alignment suggested a small deletion, but failed to precisely identify it. Aligning the same data sets with Bowtie2 in very sensitive local mode did precisely identify the deletion as a 21-bp deletion mediated by a GCGGAACC repeat in the wild-type gene. We found no mutations in the *dcp1Δ* or *dcp2Δ* strains for any of the other genes that are mutated in our evolved isolates. Similarly, analyzing the *dcp2Δ* RNA-seq data from reference (Geisler *et al.* 2012) (SRR364981), we identified the same *tl(gag)g* mutation as in our evolved isolates 4-1 and 4-2 and a novel *kap123* mutation. We did not find *kap123* mutations in wild-type controls (SRR4163289, SRR4163290, SRR4163291), *xrn1Δ* (SRR4163307, SRR4163308, SRR4163309), *dcp2-7* (SRR2045250, SRR2045251, our RNA-seq data), *dhh1Δ* (SRR6362787), *pat1Δ* (SRR6362781), *lsm1Δ* (SRR6362784), *dcp2-N245* (SRR6362793), *dcp2-N245-E153Q* (SRR6362796), *dcp2-N245-E198Q* (SRR6362799), *scd6Δ* (SRR7162931), *caf1Δ* (SRR7174202), or *dhh1Δ* (SRR3493892, SRR4418659) (Radhakrishnan *et al.* 2016; Wery *et al.* 2016; Celik *et al.* 2017; Jungfleisch *et al.* 2017; He *et al.* 2018; Webster *et al.* 2018; Zeidan *et al.* 2018). This suggests that only very severe decapping defects select for *kap123* suppressors.

Data availability

The authors state that all data necessary for confirming the conclusions presented in the article are represented fully within the article. RNA-seq data are available at the Sequence Read Archive under project number PRJNA626686. Supplemental data are available at https://doi.org/10.6084/m9.figshare.12985820. All yeast strains and plasmids used are available upon request.

Results

DCP2 is required for normal growth of yeast

Although *DCP2* is annotated as an essential gene in the Saccharomyces Genome Database (yeastgenome.org), other studies reported that *DCP2* is not an essential gene (Dunckley and Parker 1999; Giaever *et al.* 2002; Geisler *et al.* 2012; He and Jacobson 2015). The genome-wide effort to identify essential genes was based on sporulating a heterozygous diploid *DCP2/dcp2Δ* strain and attempting to recover haploid *dcp2Δ* strains. We obtained this same commercially available heterozygous diploid *DCP2/dcp2Δ* strain and repeated sporulation and tetrad dissection (Figure 1A). We expected that this would produce viable wild-type and inviable *dcp2Δ* progeny in a 1:1 ratio. However, upon prolonged growth we isolated viable *dcp2Δ* (34%) along with wild-type (51%) and inviable *dcp2Δ* progeny (14%) (Figure 1B). Although we were able to recover viable *dcp2Δ* progeny, these spores formed much smaller colonies even after prolonged incubation.

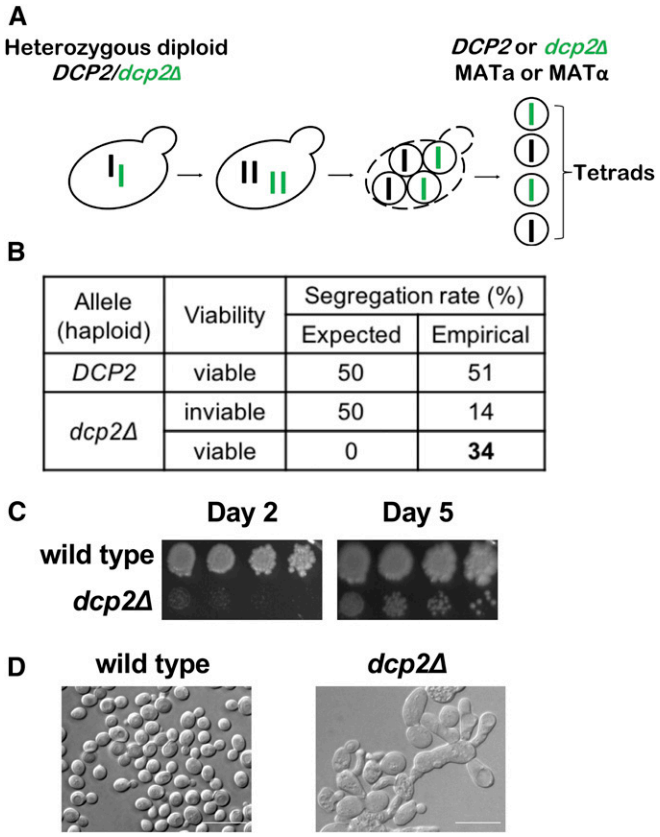

Allele (haploid)	Viability	Segregation rate (%)	
		Expected	Empirical
DCP2	viable	50	51
dcp2Δ	inviable	50	14
	viable	0	**34**

Figure 1 Isolation of viable *dcp2Δ* cells with severe growth and morphological defects. (A) Diagram of tetrad analysis of heterozygous diploid *DCP2/dcp2Δ* strain. (B) Tetrad dissection results in wild-type and *dcp2Δ* colonies. If *DCP2* is essential as annotated, 50% of the spores would be expected to be inviable. Instead 34% of the spores analyzed were *dcp2Δ* and viable. (C) *dcp2Δ* colonies resulting from tetrad dissection grow slowly. Serially diluted wild-type and viable *dcp2Δ* colonies from B were spotted on YPD solid media and grown at 30° for the indicated times. (D) *dcp2Δ* cells resulting from tetrad dissection have morphological defects. Cells were grown at 30° until OD_{600} reaches 0.3–0.4. Samples were diluted in YPD and examined by light microscopy. Bar represents 10 μm.

To further examine the growth and morphology of the recovered *dcp2Δ* strains, they were serially diluted, spotted on YPD, and cultured at 30°. Although viable, the *dcp2Δ* strains grow extremely slowly compared to wild type (Figure 1C). Examination through light microscopy revealed irregular and heterogeneous cell morphology, with many elongated cells in clumps (Figure 1D). Additionally, multiple vacuole-like organelles of different sizes accumulated in these cells. Taken together, this suggests that *DCP2* is required for normal growth and morphology of budding yeast (see *Discussion*).

Experimental evolution of dcp2Δ strains results in improved growth and morphology

To understand the function of *DCP2* that affects cell growth, we decided to identify suppressors of the growth defect of *dcp2Δ*. We used an experimental evolution approach that allows cells to accumulate mutations and enriches for suppressors that are advantageous for fitness in the absence of

DCP2. For this, we used four haploid progeny, each derived from a different tetrad (meiosis). Each haploid *dcp2Δ* strain was used to start duplicate liquid cultures. Once these cultures reached saturation, we diluted them into new media for several iterations (Figure 2A). Throughout the experimental evolution process, growth of all *dcp2Δ* populations was examined both by spotting serially diluted cultures on solid media (data not shown), and by measuring OD_{600} of cells growing in liquid media (Figure S1). During the course of the experimental evolution, we observed growth improvement at the 90th generation, and further growth improvement was observed at the 180th generation (Figure S1). However, in most cases, the growth improvement from 180 to 270 generations was minimal (Figure S1). Thus, we stopped the experimental evolution process after ~270 generations and further analyzed these *dcp2Δ* populations (evolved *dcp2Δ*). All eight evolved *dcp2Δ* populations grew better than their parental nonevolved *dcp2Δ* strain, although not as well as the wild-type strain (Figure 2B). The doubling time of the eight evolved *dcp2Δ* populations is 1.5- to 2-fold longer than that for the wild-type strain, but much shorter than the doubling time of four nonevolved *dcp2Δ* strains, which could not be calculated in the 16-hr period of the experiment because of the extremely slow growth. Similar to the growth improvement, the morphological defects in nonevolved *dcp2Δ* strains are partially restored in evolved *dcp2Δ* populations (Figure 2C and Figure S2). Evolved *dcp2Δ* cells had a more homogenous morphology, were less elongated, and less clumped compared to nonevolved *dcp2Δ* cells. These results suggest that the experimental evolution of *dcp2Δ* successfully selects suppressor mutations that confer growth improvement on *dcp2Δ* strains.

Whole-genome sequence analysis identifies suppressors of dcp2Δ growth defects

To identify suppressor mutations that confer growth improvement to *dcp2Δ* we performed whole-genome sequence (WGS) analysis on evolved *dcp2Δ* strains. We suspected that the evolved populations were genetically heterogeneous, which complicates the analysis and interpretation of WGS. Thus, for each evolved *dcp2Δ* population, we picked a single colony to generate eight genetically homogeneous evolved *dcp2Δ* isolates. As we observed in the evolved *dcp2Δ* populations, all eight evolved *dcp2Δ* isolates grew better than their nonevolved *dcp2Δ* counterparts (Figure 3A). We then sequenced the genomes of the eight evolved *dcp2Δ* isolates as well as the starting diploid *DCP2/dcp2Δ* strain (average genome coverage 112-fold), and identified mutations that were present in the evolved isolates, but not in the starting diploid (Figure 3B and Figure S3A). Each evolved *dcp2Δ* isolate contains nonsynonymous mutations in two to six genes that are not present in the heterozygous diploid *DCP2/dcp2Δ* strain. All of them were point mutations, including substitution and deletion/insertion of a small number of bases. We did not detect any larger deletions or aneuploidy (Figure S3B), which is often seen after the deletion of an essential gene (Liu *et al.* 2015).

Strikingly, all eight evolved *dcp2Δ* isolates had a mutation in the *KAP123* gene, which encodes one of the 14 karyopherins that mediate nucleocytoplasmic trafficking (Chook and Suel 2011; Aitchison and Rout 2012). In total, six different *kap123* alleles were identified from the evolved *dcp2Δ* isolates. Isolates 2-1 and 2-2 are derived from the same haploid spore and both contained the *kap123-E821X* nonsense

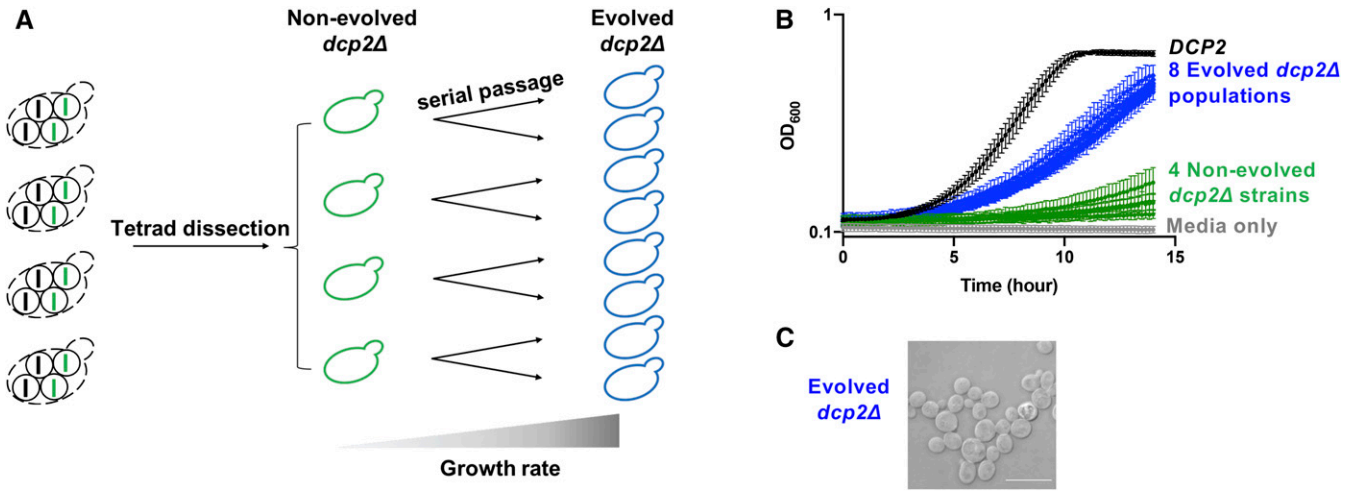

Figure 2 Experimental evolution of *dcp2Δ* strains results in growth and morphological improvement. (A) Diagram of experimental evolution. Four *dcp2Δ* strains (middle) isolated from distinct tetrads (left) were subject to serial passage. Two replicate samples of *dcp2Δ* strains were transferred to new media in iterations until the growth rate increases (right). (B) The *dcp2Δ* growth defect is partially improved in evolved *dcp2Δ* populations (blue) compared to nonevolved *dcp2Δ* strains (green). Cells were grown at 30° and OD_{600} was measured every 10 min for ~15 hr. Shown is the average OD_{600} from replicate cultures and their standard deviations, plotted on a log scale. $n = 8$ for *DCP2*, $n = 4$ for each nonevolved *dcp2Δ*, and $n = 2$ for each evolved *dcp2Δ*. (C) Morphological defects are partially restored in evolved *dcp2Δ* populations. A representative microscopic image of an evolved *dcp2Δ* population is shown. Bar represents 10 μm.

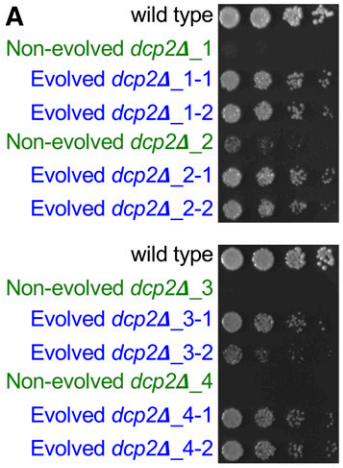

B

Evolved dcp2Δ	Recurring Genes			Other genes
	KAP123	*tL(GAG)G*	*WHI2*	
1-1	R1068S	-	L170W	*ATG22, GPA2, NUP157*
1-2	A550V	-	L170W	*ATG22, GPA2, SET1, PUF3*
2-1	E821X	-	-	*WHI4, RPO21*
2-2	E821X	nt47_T>C	-	*WHI4*
3-1	E372fs	-	Q20X	*CSE2, PSP2*
3-2	Y1018X	-	-	*CSE2, IRA1, SAR1, SGT2*
4-1	T26fs	nt25_G>T	-	-
4-2	T26fs	nt25_G>T	-	*PSR1*

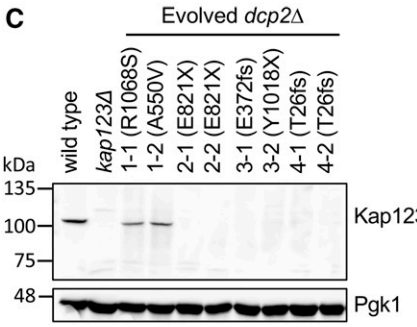

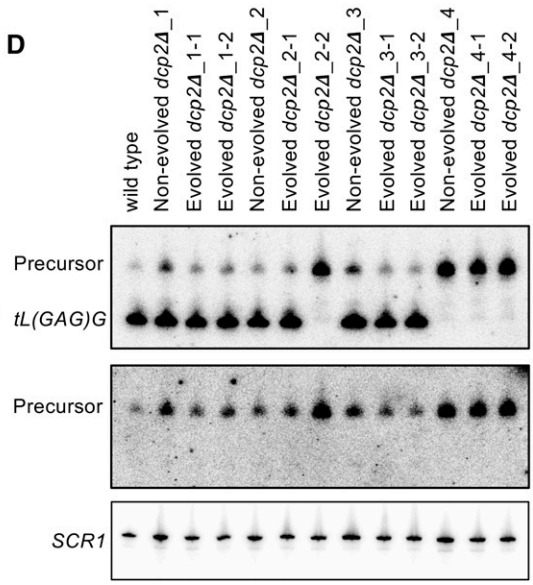

Figure 3 Whole-genome sequencing identifies multiple null mutations in *KAP123* and *tL(GAG)G*. (A) The growth defect is partially improved in evolved *dcp2Δ* isolates. A single colony was isolated from each evolved population (blue) and haploid starting strain (green). Each of these genetically homogeneous strains was serially diluted, spotted on YPD solid media, and grown at 30°. Shown is the growth at day 2. (B) Whole-genome sequences were determined for the eight evolved *dcp2Δ* isolates and compared to the *DCP2/dcp2Δ* starting diploid. Nonsynonymous mutations that are not present in the starting diploid are listed. (C) Six of the evolved isolates have null mutations in *KAP123* that generate a premature stop codon and they do not express Kap123. A representative Western blot analyzing the expression level of Kap123 (top) from the indicated strains is shown. Pgk1 (bottom) is used as loading control. (D) Three of the evolved isolates have null mutations in *tL(GAG)G* and do not express mature *tL(GAG)G* tRNA. A representative Northern blot of *tL(GAG)G* tRNA (top and middle) from the indicated strains is shown. The top panel is probed with an oligonucleotide complementary to mature *tL(GAG)G*, while the middle panel is probed with an oligonucleotide complementary to 5′ extended precursors of *tL(GAG)G*. *SCR1* is used for loading control (bottom).

mutation. We conclude that this mutation arose very early, before the duplicate cultures were started. Similarly, each pair of evolved isolates shared at least one mutation, which must have arisen early, but also differed from its sister isolate by additional mutations (see *Discussion*).

Four *kap123* mutant alleles have either a nonsense mutation or a frameshift mutation that generates a premature stop codon, and thus are likely loss-of-function mutations. Two of the mutations are missense mutations, A550V and R1068S, that both affect conserved residues that are structurally important (Figure S4A). Western blot analysis showed that the Kap123 protein was not detectable from the six evolved *dcp2Δ* isolates harboring nonsense or frameshift mutation, implying destabilization of mRNA, protein, or both. In contrast, Kap123-A550V and Kap123-R1068S were expressed (Figure 3C).

In addition to *KAP123*, we identified multiple alleles of *tL(GAG)G* and *WHI2* in our evolved isolates. *WHI2* encodes a protein involved in stress response and the TOR pathway in yeast (Kaida *et al.* 2002; Chen *et al.* 2018). One of the *whi2* alleles introduces an early stop codon (*whi2-Q20X*) and thus is likely a loss-of-function allele. The *tL(GAG)G* gene encodes leucine tRNA with a GAG anticodon, and both of the mutations are predicted to disrupt tRNA folding (Figure S4B). Northern blot analysis indicated that the mutant tRNA was not expressed (Figure 3D). In addition, pre-tRNA with 5′ extensions appeared more abundant in the mutant, suggesting that the structural perturbations in *tL(GAG)G* interfere with 5′ end processing by RNase P. The nonevolved *dcp2Δ*_4 strain did not produce the mature tRNA (Figure 3D). In addition, the two evolved *dcp2Δ* strains derived from the *dcp2Δ*_4 had the same allele, implying that this mutation had already arisen in their common ancestor strain, nonevolved *dcp2Δ*_4 (Figure S12A).

Overall, these data suggest that each of the evolved *dcp2Δ* isolates contains loss-of-function mutations in *KAP123*, *tL(GAG)G*, and/or *WHI2*, as well as other mutations of unclear significance, and that some of these mutations arose very early, whereas others arose later.

Null mutations of KAP123, tL(GAG)G, or WHI2 are sufficient to restore growth of dcp2Δ

For genes that were mutated in multiple evolved *dcp2Δ* isolates, we tested whether a null mutation of each gene is

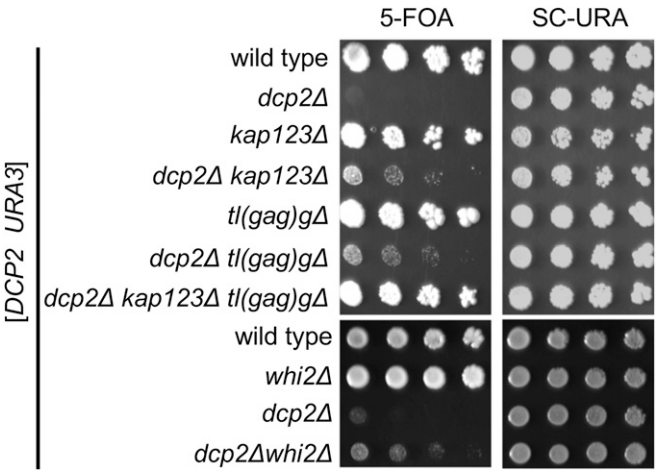

Figure 4 Null mutations of *KAP123*, *tL(GAG)G*, or *WHI2* are sufficient to suppress the growth defect of *dcp2Δ*. Growth assay showing that the extremely slow growth of *dcp2Δ* is suppressed by *kap123Δ*, *tl(gag)gΔ*, or *whi2Δ*. Null mutations of *KAP123* and *tL(GAG)G* have an additive effect on the growth. Each strain was made by sporulation of a double heterozygous diploid transformed with a *URA3* plasmid expressing *DCP2*. Haploid progeny were serially diluted and spotted on 5FOA and SC-URA (control) solid media. Shown is the growth of a representative haploid strain.

individually sufficient to suppress *dcp2Δ* growth defects. Because our WGS indicated that *dcp2Δ* strains quickly accumulated suppressors, we were careful to minimize selection for undesired spontaneous suppressors that would complicate the analysis of the desired potential suppressors [*kap123Δ*, *tl(gag)gΔ*, and *whi2Δ*]. We therefore started with the heterozygous *DCP2/dcp2Δ* diploid strain that we had sequenced, and that contained wild-type *KAP123*, *WHI2*, and *tL(GAG)G* genes. We then knocked out one of the alleles of *KAP123*, *WHI2*, or *tL(GAG)G* to generate *DCP2/dcp2Δ KAP123/kap123Δ*, *DCP2/dcp2Δ WHI2/whi2Δ*, and *DCP2/dcp2Δ tL(GAG)G/tl(gag)gΔ* diploids. Each of these three double heterozygous strains was then transformed with a plasmid that carried functional *DCP2* and *URA3* genes, and haploid progeny were generated and genotyped. Finally, the strains were grown on media lacking uracil (selecting for the *DCP2 URA3* plasmid) or media containing 5FOA (counter-selecting against the *DCP2 URA3* plasmid). Growth on 5FOA-containing media in this assay indicates that the strain is viable in the absence of the *DCP2* plasmid. This elaborate experimental setup allowed us to determine growth without inadvertently preselecting for suppressor mutations.

As expected, progeny with a functional chromosomal *DCP2* gene derived from each of the double heterozygotes readily formed colonies on 5FOA (Figure 4), indicating that they could grow after losing the *DCP2 URA3* plasmid. In contrast, the *dcp2Δ* progeny derived from each of the double heterozygotes failed to form colonies on 5FOA after up to 5 days of incubation. Importantly, *dcp2Δ kap123Δ*, *dcp2Δ whi2Δ*, and *dcp2Δ tl(gag)gΔ* strains each formed small colonies on 5FOA-containing media, indicating that they were able to grow after losing the *DCP2* plasmid. Thus, each of these null alleles is sufficient to suppress the *dcp2Δ* growth phenotype.

Multiple studies have reported inadvertent mutations of *WHI2* in various yeast knockout strains (Lang *et al.* 2013; Teng *et al.* 2013; Comyn *et al.* 2017). In contrast, we could not find any other studies identifying *kap123* or *tl(gag)g* as suppressors. Thus, the effect of *whi2Δ* on *dcp2Δ* appears to be less specific than the other two suppressors. Therefore, we decided to focus on *KAP123* and *tL(GAG)G* for further analyses.

To test whether *kap123Δ* and *tl(gag)gΔ* suppressed *dcp2Δ* growth defects through a common mechanism, we generated *dcp2Δ kap123Δ tl(gag)gΔ* triple mutant with the *DCP2 URA3* plasmid. Importantly, the triple mutant grew better on 5FOA plates than either double mutant (Figure 4), indicating that *kap123Δ* and *tl(gag)gΔ* act independent of each other to improve *dcp2Δ* growth. This observation that multiple suppressors further improve growth also explains why the experimental evolution resulted in strains with multiple mutations.

Other viable dcp2Δ or dcp1Δ strains contain similar suppressor mutations

Our WGS data suggest that *DCP2* is required for growth under laboratory conditions, but some previous studies have reported that *DCP2* is dispensable for survival. Some studies have attributed these differences to the use of different strains, *e.g.*, it has been reported that *dcp2Δ* is viable in the W303 strain but lethal in S288C (He *et al.* 2014; He and Jacobson 2015). However, the available genome sequences of W303 and S288C revealed that neither contains obvious null mutations in *KAP123*, *WHI2*, or *tL(GAG)G*. We therefore reanalyzed the strains used in three different studies.

First, we analyzed published RNA-seq data of a *dcp2Δ* strain in the S288C background to reveal mutations shown as mismatches between the RNA reads and reference genome (Geisler *et al.* 2012). The *dcp2Δ* strain used in that study (yJC327 in Figure S12A) was obtained from our laboratory and is derived from the nonevolved strain *dcp2Δ*_4 used in our studies. Our WGS data above indicated that nonevolved strain *dcp2Δ*_4 strain had an early arising *tl(gag)g-G25U* allele and, as expected, we detected this allele in the RNA-seq reads. This result confirms the Northern blot result above that nonevolved strain *dcp2Δ*_4 lacks mature *tL(GAG)G* tRNA. In addition, we detected a *kap123-T766fs* allele in the RNA-seq data that is different from mutations what we identified in WGS analysis. Thus, this strain acquired the *tl(gag)g* mutation at some point before we shared it, and acquired an additional *kap123* mutation at some point before the RNA-seq was performed (Figure S12A).

We also reanalyzed publicly available RNA-seq data for the previously reported viable *dcp2Δ* and *dcp1Δ* mutants in the W303 strain background (Celik *et al.* 2017). Importantly, all of the reads from the *dcp2Δ* strain that mapped to codon 786 of *KAP123* indicated that this codon was a UAA codon instead of a UAC codon (Figure S5A). We conclude that the

dcp2Δ strain used in this RNA-seq experiment is a *dcp2Δ kap123-Y687X* double mutant. Similarly, in the *dcp1Δ* strain, we detected a 21-nt deletion in *KAP123* (*kap123-Δ510-516*; Figure S5B). Moreover, the RNA reads from the control W303 strain indicated that it contained a wild-type *KAP123* gene. Thus, the *kap123* mutations in the *dcp1Δ* and *dcp2Δ* strains are not inherent differences between W303 and S288C, but are instead mutations that inadvertently arose in the mutant strains.

Lastly, much of the initial investigations of decapping were carried out in a yRP strain background, and *dcp2Δ* was described as viable in this background (Beelman *et al.* 1996; Dunckley and Parker 1999). We therefore PCR amplified and sequenced the *KAP123* gene from this *dcp2Δ* strain (yRP1346) and detected that the PCR product was a mixture of *kap123-G727X* and *KAP123*. Thus, a *kap123* mutation appeared to have arisen after this *dcp2Δ* strain was created.

Overall, these results indicate that many of the previously reported viable *dcp2Δ* strains contain previously undetected mutations in *KAP123* that likely contribute to their growth. We conclude that suppressors of the *dcp2Δ* slow growth phenotype readily occur in diverse strain backgrounds and have contributed to different conclusions on the essentiality of *DCP2* (see *Discussion*).

Effect of decapping defects on KAP123 expression

Although most genes in *S. cerevisiae* can be overexpressed, some "dosage-sensitive" genes cause growth defects upon overexpression. *KAP123* is among the most dosage-sensitive genes (Makanae *et al.* 2013). Thus, we considered the possibility that decapping is critical to maintain the *KAP123* mRNA and Kap123 protein at a low nontoxic level. A *dcp2Δ* strain would thus be lethal because Kap123 is overexpressed to toxic levels, and a *kap123* mutation would restore growth. We tested this possibility using two different approaches. Because all of our *dcp2Δ* strains contain *kap123* mutations, we used a *dcp2-7* temperature sensitive strain, which has a wild-type *KAP123* gene (see *Materials and Methods*) and performed Western blot analysis. The decapping enzyme in a *dcp2-7* strain can be inactivated rapidly by growing it at room temperature and then incubating it at 37° (van Hoof *et al.* 2000; Dunckley *et al.* 2001; Schaeffer *et al.* 2008; Wery *et al.* 2016) (see Figure 7C and Figure 8 below). This showed that Kap123 was not overexpressed upon Dcp2 inactivation (Figure 5). We also checked the *KAP123* levels in the RNA-seq data from *dcp2-7* and *dcp1Δ* strains (Wery *et al.* 2016; Celik *et al.* 2017). The *dcp2-7* strain contains a wild-type *KAP123* allele, and although the *dcp1Δ* contains a *kap123* mutation, this in frame deletion is not expected to affect *KAP123* mRNA stability. Consistent with our Western blot, neither decapping mutant strain had an increased *KAP123* mRNA level (Figure S6A). These results indicate that suppression of the growth phenotype of Dcp2 is not through reducing *KAP123* expression below a toxic level.

The GAG anticodon of tL(GAG)G determines the genetic interaction with DCP2

The *tl(gag)gΔ* that affects growth of *dcp2Δ* affects one specific tRNA gene out of the 275 tRNA genes in the yeast genome. This suggests that this tRNA must have some unique feature that governs the *dcp2Δ* genetic interaction. We therefore determined what sequence elements of *tL(GAG)G* are important for genetic interaction with *dcp2Δ*. We focused on the nucleotides that are different between *tL(GAG)G* and other leucine tRNAs. There are 12 nucleotides that distinguish *tL(GAG)G* from other leucine tRNAs. Eight of these replace one base pair with another and seem unlikely to affect tRNA function. The other four are three nucleotides in the anticodon loop (C33, U34, and U38) and A57 in the ψ loop (Figure S4B). Thus, either the anticodon loop or A57 of *tL(GAG)G* were replaced by the corresponding nucleotides from a different leucine tRNA [*tL(UAG)*]. Northern blot analysis indicated that both of these mutant tRNAs were expressed similarly to wild-type *tL(GAG)G* (Figure 6A), but caused different growth phenotypes (Figure 6B). When the A57G mutant was introduced into a *dcp2Δ kap123Δ tl(gag)gΔ* strain, the growth phenotype was similar to that of wild-type *tL(GAG)G*. It is important that restoration of *tL(GAG)G* function reverses the suppression phenotype and thus reduces growth rate. This reduced growth rate is clearly seen for wild-type *tL(GAG)G* and the A57G mutant, when compared to the empty vector control (Figure 6B). Thus, while A57 distinguishes *tL(GAG)G* from other Leu tRNAs, it is not relevant to the genetic interaction with *dcp2Δ*. In contrast, the anticodon loop mutant behaved similar to empty vector in this growth assay, and different from the wild-type *tL(GAG)G*

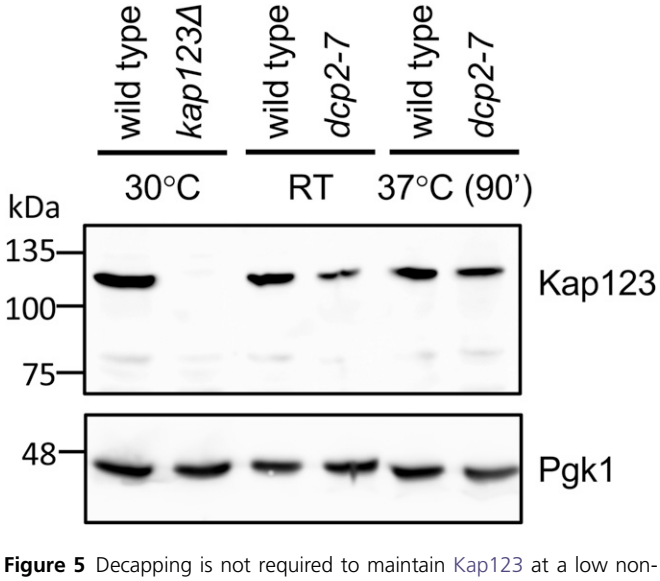

Figure 5 Decapping is not required to maintain Kap123 at a low nontoxic level. Expression of Kap123 is not increased in decapping deficient cells. A representative Western blot analyzing the expression of Kap123 (top) is shown. Pgk1 (bottom) is used a loading control. Lane 1–2: cells were grown at 30°; lane 3–4: cells were grown at room temperature (RT); lane 5–6: cells were grown at RT until OD_{600} reached 0.6–0.8, then transferred to 37° for 90 min.

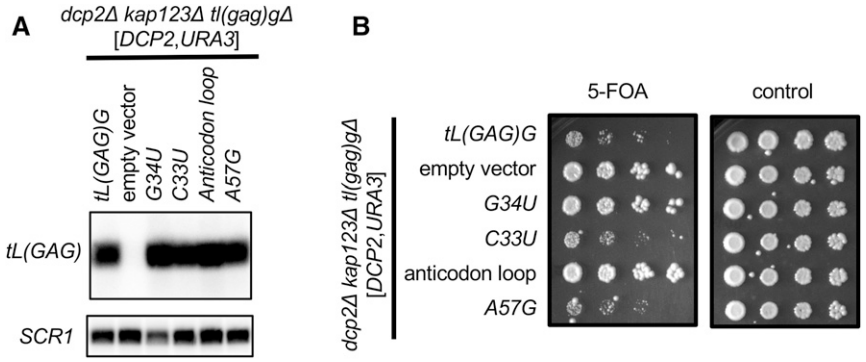

Figure 6 The GAG anticodon of *tL(GAG)G* affects growth of *dcp2* implicating a mechanism that involves translation of CUC and CUU codons. A *dcp2Δ kap123Δ tl(gag)gΔ* strain harboring a *DCP2*, *URA3* plasmid was transformed with wild-type or mutant *tL(GAG)G* plasmids, or an empty vector control. (A) Northern blot showing that each tRNA is expressed at similar levels. The blot was probed with a probe that is specific for *tL(GAG)G* and unaffected by any of the mutations (top) or for *SCR1* as a loading control (bottom). (B) The strains were plated on 5-FOA plates (left) showing that the wild-type, C33U, and A57G tRNAs complemented the effect of *tl(gag)gΔ*, but empty vector, G34U, and changing the whole anticodon loop (including G34U) did not. In the presence of *DCP2* (right panel), none of the mutations affected growth.

gene. Therefore, the specific sequence of the anticodon stem loop is critical for the genetic interaction with *dcp2Δ*.

To further narrow down what nucleotides within the anticodon loop are critical, we focused on two striking differences. First, *tL(GAG)G* is the only tRNA with a C33, the position immediately preceding the anticodon. All 274 other yeast tRNAs have U33, and U33 is important for efficient translation (Santos *et al.* 1996; Silva *et al.* 2007), presumably because it is critical to from the "U-turn" three-dimensional structure that makes the anticodon available to base pair with the codon. We thus changed C33 in *tL(GAG)G* to U33 to match all other tRNAs. This allele was expressed similar to wild type and affected growth of the *dcp2Δ kap123Δ tl(gag)gΔ* strain, like wild-type *tL(GAG)G* (Figure 6, A and B). Thus, while C33 is unique to *tL(GAG)G*, it is also not relevant to the *dcp2Δ* genetic interaction. The other striking difference between the anticodon loop of *tL(GAG)G* and other Leu tRNAs is, of course, the anticodon itself. We therefore changed the first anticodon nucleotide (G34) to a U, to match the sequence of the three *tL(UAG)* genes. Northern blot analysis showed that the level of this mutant tRNAs is comparable to wild-type *tL(GAG)G* (Figure 6A). Interestingly, when we compared growth, the mutant tRNA with a UAG anticodon behaved similar to an empty vector control and different from the wild-type *tL(GAG)G* (Figure 6B). Because the GAG is crucial for the genetic interaction with *DCP2*, we suggest that the mechanism of suppression is to alter translation at (some) CUC or CUU codons.

Suppressor mutations of dcp2Δ do not restore mRNA decay to normal rates

We next used several assays to determine whether the suppressor mutations affected mRNA decay rates or pathways. First, we examined whether the 5′ to 3′ decay pathway is restored in the evolved *dcp2Δ* isolates. Several other enzymes carry out activities that are similar to Dcp2, including Dcs1, Dxo1, Rai1, and the L-A viral GAG protein. Specifically, Dcs1 cleaves the cap structure that remains after the mRNA is degraded in the 3′ to 5′ direction, Dxo1 and Rai1 digest aberrant caps, and GAG transfers the cap from cellular mRNAs to viral RNA (Blanc *et al.* 1994; Liu *et al.* 2002; Xiang *et al.* 2009; Jiao *et al.* 2010; Fujimura and Esteban 2011; Chang *et al.* 2012; Doamekpor *et al.* 2020). Although none of these enzymes have canonical functions for 5′ to 3′ decay of bulk cytoplasmic mRNA, it appeared possible that our suppressor mutations redirect their activities. To test this possibility, we compared the directionality of mRNA decay *in vivo* among wild-type, nonevolved, and evolved *dcp2Δ* isolates. In this assay, we used an mRNA with a G-quadruplex structure in the 3′ UTR. This structure impedes Xrn1, and therefore any decapping and 5′ to 3′ decay results in the accumulation of a decay intermediate that is easily detectable by Northern blotting (Muhlrad *et al.* 1994). This decay intermediate was undetectable in Northern blots from both the nonevolved and evolved *dcp2Δ*, while this intermediate was abundant in the wild-type control (Figure 7A, quantitated in Figure S7). This result demonstrates that the evolved *dcp2Δ* strains are still defective in 5′ to 3′ degradation, at least in this widely used model mRNA.

In addition to exonucleases, some endonucleases have been shown to contribute to cytoplasmic mRNA decay in yeast. For example, Ire1 and tRNA splicing endonuclease (TSEN) cleave specific mRNAs (Sidrauski and Walter 1997; Tsuboi *et al.* 2015). One possibility is that our suppressors increase activity or decrease the specificity of some endonuclease. We also entertained the idea that *tl(gag)g* mutations could cause stalling of translating ribosomes, which might trigger "no-go" cleavage by Cue2 (Doma and Parker 2006; D"Orazio *et al.* 2019). Regardless of the endonuclease involved, endonucleolytic cleavage of the mRNA upstream of the G-quadruplex initiates Xrn1-mediated decay and leads to the same decay 5′ to 3′ decay intermediate as decapping (Doma and Parker 2006; Tsuboi *et al.* 2015; Cherry *et al.* 2019; D'Orazio *et al.* 2019). Therefore, the undetectable level of this decay intermediate indicates that the suppressors do not increase endonucleolytic decay of *MFA2pG* mRNA.

Second, it has previously been shown that if the 5′ to 3′ decapping pathway is impaired, the RNA exosome and its

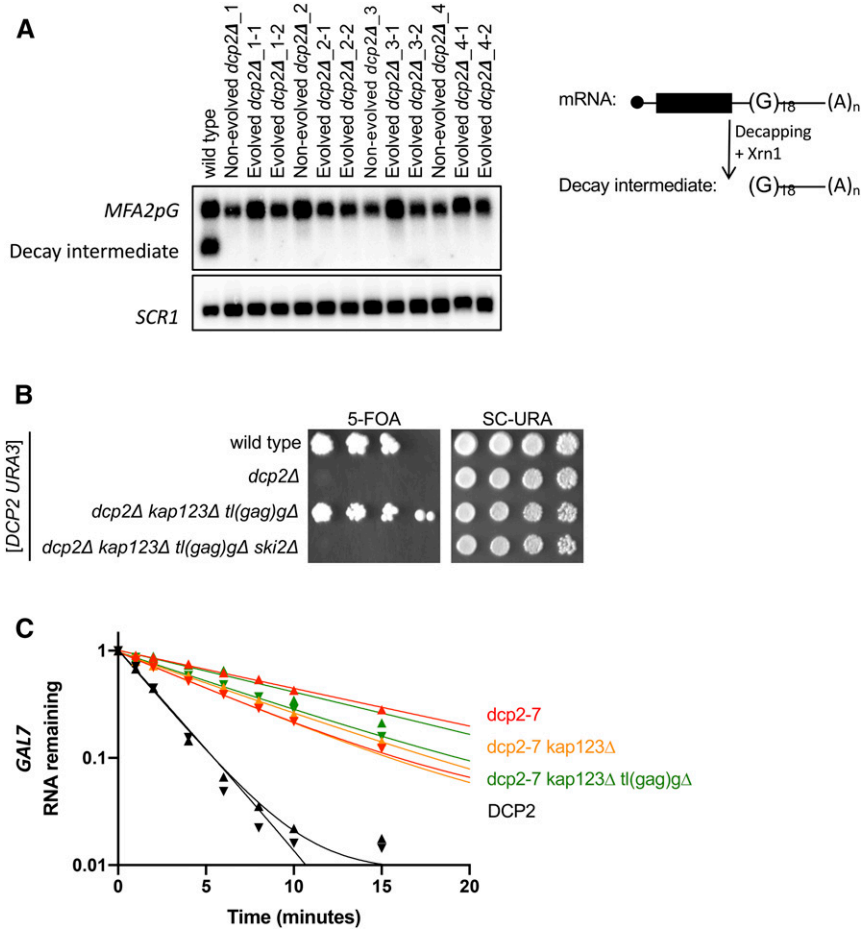

Figure 7 Suppressor mutations of *dcp2Δ* do not restore mRNA decay. (A) 5′ to 3′ mRNA decay is defective in evolved *dcp2Δ* strains. Each strain was transformed with an *MFA2pG* reporter (right). Decapping, or endonucleolytic cleavage, followed by 5′ exonucleolytic decay of *MFA2pG* produces a decay intermediate that is a sensitive measure of decapping. Total RNA was isolated, and *MFA2pG* mRNA was analyzed by Northern blotting. A representative blot from three replicates is shown. Top panel was probed for *MFA2pG*, and the bottom panel for the loading control *SCR1*. Quantitation of all three replicates is in Figure S7. (B) RNA exosome-mediated decay is required in *dcp2Δ* suppressor mutants. *dcp2Δ kap123Δ tl(gag)gΔ* is no longer viable in the absence of *SKI2*. Each strain was made by sporulation of a quadruple heterozygous diploid transformed with a *URA3* plasmid expressing *DCP2*. Haploid progeny were serially diluted and spotted on 5FOA and SC-URA (control) solid media. Shown is the growth of a representative haploid strain at day 5. (C) The stability of *GAL7* mRNA is unaffected by *kap123Δ* and/or *tl(gag)gΔ* in *DCP2*-deficient cells. Cells exponentially growing at 21° in galactose were transferred to 37° for 1 hr. Transcription of *GAL7* was repressed by the addition of dextrose at time 0, and cells were harvested at multiple time points. Total RNA was isolated and *GAL7* mRNA levels were analyzed by Northern blotting. Plotted is remaining *GAL7* mRNA levels relative to *SCR1* levels of two biological replicates. Data point triangles are pointing up for one replicate, and down for the other.

associated helicase Ski2 become rate limiting for mRNA decay (Anderson and Parker 1998). This is reflected in growth phenotypes. Specifically, *ski2Δ* does not cause an obvious growth defect if Dcp2 is fully functional, but is lethal if decapping activity is impaired (Anderson and Parker 1998). We therefore combined *ski2Δ* with *dcp2Δ kap123Δ tl(gag)gΔ*. As before, the *dcp2Δ kap123Δ tl(gag)gΔ* triple mutant is viable, but the *dcp2Δ kap123Δ tl(gag)gΔ ski2Δ* quadruple mutant is inviable (Figure 7B), indicating that cytoplasmic RNA exosome activity is required even in the presence of *dcp2Δ* suppressors. This suggests that the RNA exosome is the major mRNA-degrading activity in the *dcp2Δ kap123Δ tl(gag)gΔ* mutant. Overall, the *MFA2pG* assay and the *ski2* synthetic lethality indicate that *kap123Δ* and *tl(gag)gΔ* do not result in hyperactivation of a novel mRNA degradation pathway.

Third, we tested the effect of *kap123Δ* and *tl(gag)gΔ* on stability of three specific mRNAs. Because all our *dcp2Δ* strains already have suppressor mutations, we again used the temperature-sensitive *dcp2-7* allele in this experiment and compared the stability of the *GAL7*, *GAL1*, and *GAL10* mRNAs in a *dcp2-7* strain to their stability in *dcp2-7 kap123Δ* and *dcp2-7 kap123Δ tl(gag)gΔ* strains. For this experiment, the expression of the *GAL* mRNAs was induced by growth in the presence of galactose, the decapping enzyme was then inactivated by incubating the cultures at 37°. Finally, dextrose was added to inhibit transcription from the *GAL* genes, and RNA was isolated in a time course and analyzed by Northern blotting (Figure S8A). This revealed that the *GAL* mRNAs were each degraded more slowly in the *dcp2-7* strain compared to a *DCP2* control, as expected (Anderson and Parker 1998; Dunckley and Parker 1999). However, when comparing the *dcp2-7 kap123Δ* and *dcp2-7 kap123Δ tl(gag)gΔ* mutants to *dcp2-7*, we detected no differences (Figure 7C and Figure S8B). In both of the suppressed strains, the mRNA half-lives were similar to the *dcp2-7* single mutant, and more stable than the wild-type control.

Taken together, these results show that unlike previously isolated suppressors (Dunckley and Parker 1999; Dunckley *et al.* 2001; Kshirsagar and Parker 2004; Segal *et al.* 2006), our suppressor mutations do not restore decapping or mRNA decay rates to wild-type levels, although we cannot exclude that they have some very small effects on mRNA degradation, or only affect specific mRNAs beyond the ones we tested. Instead, while *kap123Δ* and *tl(gag)gΔ* affect the growth of *dcp2Δ* dramatically they do not have a similar dramatic effect on cytoplasmic mRNA decay.

Suppressors have minor effects on mRNA and noncoding RNA defects in a dcp2 mutant

To gain a better understanding of how *dcp2Δ* suppressors affect the transcriptome, we performed global gene expression analysis. Biological triplicates of wild type, *dcp2-7*, *dcp2-7 kap123Δ*, and *dcp2-7 kap123Δ tl(gag)gΔ* were subjected to RNA-seq analysis after enrichment of poly(A)$^+$ RNAs. As previously reported, *dcp2-7* causes widespread disruption of the transcriptome (Wery *et al.* 2016). In our analysis, the *dcp2-7* strain shows 1004 annotated genes significantly upregulated by ≥2-fold (adjusted *P*-value < 0.05) and 618 annotated genes significantly downregulated by ≥2-fold (Figure 8A). As in previous analysis, similar numbers of genes were up- and downregulated, which we interpret to indicate that the effects are dominated by indirect effects, instead of reflecting altered stability. We did not note any particular gene or group of genes that could explain the morphological and growth phenotypes of *dcp2Δ*. A similar but slightly lower number of genes were affected in the *dcp2-7 kap123Δ* mutant, where 972 annotated genes were upregulated by ≥2-fold and 550 annotated genes were downregulated ≥2−fold compared to wild type (Figure 8B). Even fewer significant changes in the global transcripts levels were detected in the *dcp2-7 kap123Δ tl(gag)gΔ* mutant, where 752 annotated genes were upregulated by ≥2-fold and only 340 annotated genes were downregulated by ≥2-fold (Figure 8C). However, even the triple mutant showed widespread defects. We interpret these results to indicate that the suppressors have modest effects on the transcriptome.

To determine whether specific genes were affected by *kap123Δ* and *tl(gag)gΔ*, we compared the gene expression profile of *dcp2-7 kap123Δ* and *dcp2-7 kap123Δ tl(gag)gΔ* to the *dcp2-7* strain. Unlike the comparison to wild type (Figure 8, B and C), there are only a few genes differentially expressed. In *dcp2-7 kap123Δ* mutant, there were only 10 annotated genes upregulated by ≥2-fold and 20 annotated genes downregulated by ≥2-fold (Figure 8D) when compared to the single mutant *dcp2-7*. In the *dcp2-7 kap123Δ tl(gag)gΔ* mutant, 102 annotated genes were upregulated by ≥2-fold and 201 annotated genes downregulated by ≥2-fold compared to *dcp2-7* (Figure 8E). Thus, suppression of growth defects is accomplished without major effects on the transcriptome.

To determine whether the suppression mechanism engages the regulation of certain biological processes or cellular functions, we examined if any specific biological processes are enriched in transcripts whose expression significantly changed at least twofold (adjusted *P*-value < 0.05 of DESeq2) via GO enrichment analysis (Figures S9 and S10). Interestingly, the only GO category enriched in transcripts downregulated in *dcp2-7 kap123Δ tl(gag)gΔ* relative to *dcp2-7* is ribosomal RNA modification. This was particularly striking because this GO category was upregulated in *dcp2-7* compared to wild type. This GO category therefore correlated with the growth effect: it was upregulated in the *dcp2-7* mutant, and partially, but not completely, restored in the triple mutant. The genes in this GO category that were affected were mostly small nucleolar RNA (snoRNA) encoding genes. Thus, snoRNA genes are significantly dysregulated in *dcp2-7* compared to wild type and this dysregulation is partially alleviated in suppressor strains. This effect on snoRNA genes may be either a cause or an effect of improved growth.

To better understand the effect on snoRNA genes, we looked at subsets of these genes. snoRNAs can be classified by function and conserved elements into C/D box snoRNAs that direct RNA methylation, and H/ACA snoRNAs that direct pseudouridylation of RNA, and both classes of snoRNAs appeared to be affected. snoRNAs can also be divided by gene organization into monocistronic, polycistronic, and intron-encoded snoRNAs. Each of these categories is processed, but Dcp2 is not thought to play a role in snoRNA processing. Instead, the monocistronic snoRNAs are transcribed independently as ^{7m}G capped precursors. These pre-snoRNAs are then 5′ matured into ^{2,2,7m}G-capped snoRNAs by further methylations (Mouaikel *et al.* 2002), or into a 5′ phosphorylated snoRNA by cleavage by the endonuclease Rnt1 and the exonuclease Rat1 (Chanfreau *et al.* 1998a; Lee *et al.* 2003). Similarly, polycistronic precursors are separated into individual snoRNAs by Rnt1, and then 5′ processed by Rat1 (Chanfreau *et al.* 1998b; Qu *et al.* 1999). Finally, intron-encoded snoRNAs are processed from the spliced out and debranched intron (Ooi *et al.* 1998). Both polycistronic (Figure 9, A and B) and monocistronic (Figure 9, A and C) snoRNA loci were upregulated in *dcp2-7*, but most intron-encoded snoRNA loci were not (Figure 9, A and D). Moreover, inspection of read coverage at snoRNA loci indicated that what we detected was an upregulation of transcripts from snoRNA loci that were 5′ and/or 3′ extended, rather than the mature snoRNAs (Figure 9, B and C). Importantly, the loci for both uncapped (Figure 9B) and capped (Figure 9C) mature snoRNAs were affected. These observations indicate that the defect does not reflect a direct role of Dcp2-mediated decapping in snoRNA processing.

To quantitate the effect of the suppressors, we compared the log2 (fold change) of *dcp2-7* relative to wild type *vs.* that in *dcp2-7 kap123Δ* or *dcp2-7 kap123Δ tl(gag)gΔ* relative to wild type. Transcripts that were affected in both mutants (relative to wild type) were plotted. Specifically, of the 77 annotated snoRNA genes 53 were significantly affected in both *dcp2-7* (relative to wild type) and *dcp2-7 kap123Δ* (relative to wild type) (Figure 9E). If the *kap123Δ* had no effect, this should result in data points along a line with a slope of 1 (Figure 9E, gray dashed line). On the other hand, complete restoration of the *dcp2-7* defect would result in a line with a slope of 0. Of the 53 analyzed snoRNA transcripts, 87% are in between these two expectations: they were changed less in the *dcp2-7 kap123Δ* strain (Figure 9E and Figure S11C). On the other hand, 13% were more affected. Linear regression of the data revealed a slope of 0.87 with a high correlation coefficient ($R^2 = 0.90$), indicating that the snoRNA transcripts typically were decreased 13% in the double mutant relative

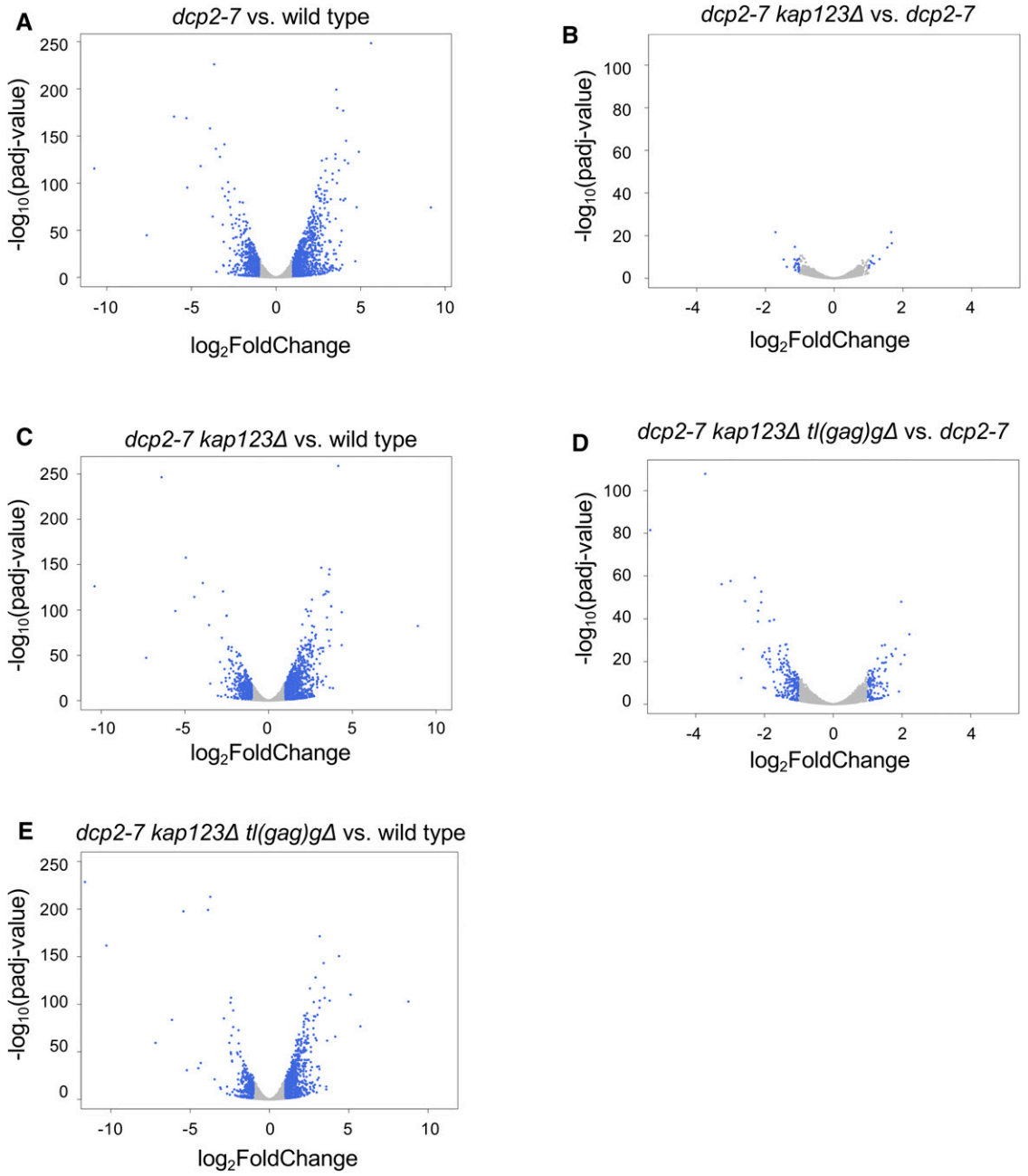

Figure 8 Transcriptome analysis of *dcp2* mutants. (A–C) Volcano plots showing differential expression of 7127 annotated genes in *dcp2-7* mutants *vs.* wild type. (D and E) Volcano plots showing differential expression of 7127 annotated genes in *dcp2-7* suppressor mutants *vs. dcp2-7* strain. (A–E) Transcripts that significantly changed at least twofold (adjusted *P*-value < 0.05) are in blue. Note the difference in scales between panels A to C and D and E.

to the *dcp2-7* single mutant (Figure 9E). The same analysis of the triple mutant showed a similar but more pronounced effect (Figure 9F and Figure S11C). These results show that snoRNA gene misregulation is less pronounced in the suppressed strains than in the *dcp2-7* single mutant cells.

Although snoRNAs were enriched among genes whose expression was increased in *dcp2-7* and partially restored in *dcp2-7 kap123Δ tl(gag)gΔ*, we sought to determine whether this effect was restricted to snoRNAs. With this goal in mind we repeated the analysis of log2 (fold change) in *dcp2-7 vs.* the suppressed strains for annotated genes, which are mostly protein-coding genes (Figure 10, A and B), and for XUTs (Figure 10, C and D). XUTs are noncoding RNAs transcribed by RNA polymerase II and increased in abundance upon *xrn1Δ* (van Dijk *et al.* 2011). Because XUTs are transcribed by RNA polymerase II, they should be capped, and thus have to be decapped before they can become Xrn1 substrates. This analysis revealed that the disruption of mRNAs and XUTs that are misregulated in both *dcp2-7* and *dcp2-7 kap123Δ tl(gag)gΔ* strains are less misregulated in the triple mutant. A total of

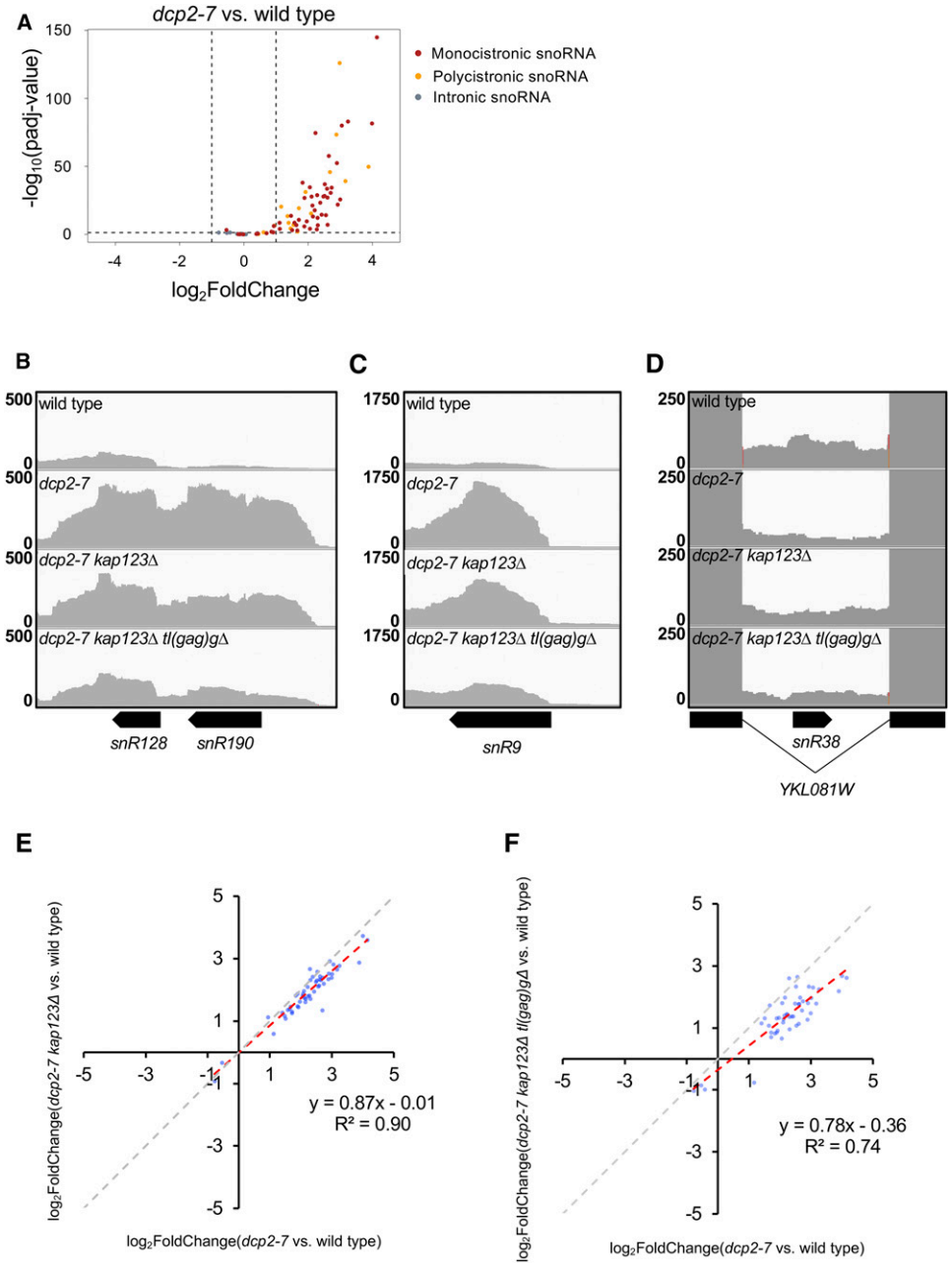

Figure 9 Suppressors ameliorate expression defects from snoRNA loci in *dcp2-7* mutant. (A) The expression of mono- and polycistronic snoRNA loci are upregulated in *dcp2-7* mutant. A volcano plot showing differential expression of snoRNA genes in *dcp2-7* strain *vs.* wild type. Monocistronic snoRNA are in red, polycistronic snoRNA genes are in orange, and intronic snoRNA genes are in gray. Dashed lines represent cut-off values for a twofold change in gene expression, and adjusted *P*-value < 0.05. (B–D) Upregulation of mono- and polycistronic snoRNA loci in *dcp2-7* mutant were reduced by *kap123Δ*, and further by *kap123Δ tl(gag)gΔ*. RNA-seq read coverage for the snoRNA gene loci *snR128-snR190* (dicistronic), *snR9* (monocistronic), and *snR38* (intronic) are shown. (E and F) Defective snoRNA expression in *dcp2-7* mutant was alleviated by *kap123Δ* and further by *kap123Δ tl(gag)gΔ*. Plotted is the differential expression of snoRNA loci in suppressor mutants *vs. dcp2-7* mutant (relative to wild type). Of 77 snoRNA genes in *S. cerevisiae*, 53 and 49 transcripts that are statistically significant (adjusted *P*-value < 0.05 of DESeq2) were plotted, respectively. The gray dashed line with slope 1 is the predicted outcome if *kap123Δ* and *tl(gag)gΔ* had no effect. The red dashed line with slope < 1 depicts linear regression analysis results.

69% of analyzed mRNA transcripts were less affected in *dcp2-7 kap123Δ tl(gag)gΔ* than in *dcp2* (Figure S11A). Similarly, 66% of analyzed XUTs changed less in the triple mutant than in *dcp2-7* compared to wild type (Figure S11B). The double mutant had similar effect of mRNAs and XUTs as the triple mutant, although the effect was slightly reduced.

Overall, our data showed that *dcp2-7* has large effects on a variety of RNAs including both mRNAs and noncoding RNAs such as snoRNAs (which are not Dcp2 substrates) and XUTs (which are Dcp2 substrates), and that the double and triple mutants had similar but slightly less disturbed transcriptomes. Furthermore, since it is hard to envision how a tRNA directly affects noncoding RNAs such as snoRNAs and XUTs, we suspect that the suppressors indirectly affect transcriptome dysregulation.

Discussion

Dcp2 is required for continuous growth

Cytoplasmic mRNA turnover is an important process that regulates gene expression, and Dcp2 carries out a key step. Previous studies have described *DCP2* as either an essential gene or a nonessential gene, and in some cases the difference has been attributed to a genetic difference between the two widely used yeast strains, S288C and W303 (Dunckley and

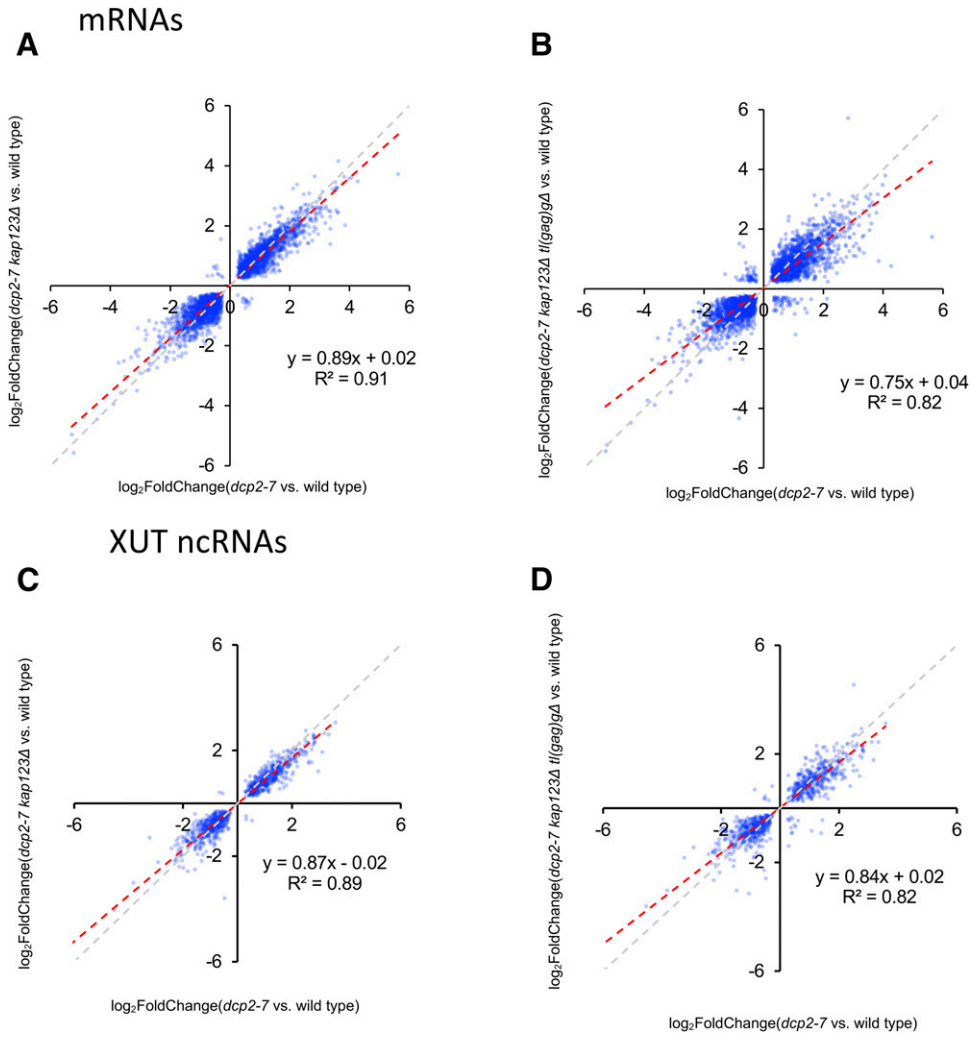

Figure 10 Suppressors ameliorate defects in expression of protein coding mRNA and XUT noncoding RNA in *dcp2-7* mutant. (A and B) Defective mRNA expression in *dcp2-7* mutant was alleviated by *kap123Δ* and further by *kap123Δ tl(gag)gΔ*. Plotted is the differential expression of mRNA loci in suppressor mutants *vs.* *dcp2-7* mutant (relative to wild type). Of 6691 mRNA genes in *S. cerevisiae*, 3236 and 3302 transcripts that are statistically significant (adjusted *P*-value $<$ 0.05 of DESeq2) were plotted, respectively. *YBR115C*, *YCR097W*, *YEL021W*, *YNL145W*, *YER110C*, and *YPL187W* are not plotted. (C and D) Defective XUT expression in *dcp2-7* mutant was alleviated by *kap123Δ*, and further by *kap123Δ tl(gag)gΔ*. Plotted is the differential expression of XUT loci in suppressor mutants *vs.* *dcp2-7* mutant relative to wild type. Of 1658 XUT genes in *S. cerevisiae*, 948 and 898 transcripts that are statistically significant (adjusted *P*-value $<$ 0.05) were plotted, respectively. (A–D) The gray dashed line with slope 1 is the predicted outcome if *kap123Δ* and *tl(gag)gΔ* had no effect. The red dashed line with slope $<$ 1 depicts linear regression analysis results.

Parker 1999; Giaever *et al.* 2002; Geisler *et al.* 2012; He and Jacobson 2015). Our studies indicate that very slow-growing *dcp2Δ* strains can be generated, but that suppressor mutations that improve growth readily occur. We further show that previous studies have inadvertently used *dcp1Δ* or *dcp2Δ* strains that contain spontaneous *kap123* suppressors. However, similar analysis from other *dcp2* alleles (*e.g.*, *dcp2-7* and *dcp2-N245*; Wery *et al.* 2016; He *et al.* 2018) and strains with mutations in decapping regulators (*lsm1Δ*, *pat1Δ*, *etc.*; He *et al.* 2018) indicated that they contained a wild-type *KAP123* gene. This suggests that only very severe decapping defects select for *kap123* mutations.

The starting *DCP2/dcp2Δ* heterozygote used in our tetrad analysis does not contain these suppressors, but a large fraction of the resulting haploid colonies do. It appears implausible that ungerminated and metabolically inactive spores accumulate suppressor mutations to high frequency, without accumulating a large number of other random mutations. Therefore, we conclude that *dcp2Δ* spores are capable of germinating and dividing for several generations. Strong selective pressure during early generations leads to the selection for suppressors that then allow further growth. The mutation rate in rapidly growing diploid yeast cells has been measured as 1.67×10^{-10} per base pair per cell doubling (Zhu *et al.* 2014). There are $\sim 10^6$ cells in a yeast colony, and the *KAP123* gene is 3342-bp long. Thus, the chance that a colony formed by a *KAP123* cell contains a cell with a *kap123* mutation is $\sim$0.6 ($1.67 \times 10^{-10} \times 10^6 \times 3342$). We suspect that the much longer generation time of *dcp2Δ* allows for more mutations to occur per generation. It thus appears that a normal or slightly elevated mutation rate, combined with strong selection, is sufficient for an initial suppressor to arise. The need for an initial suppressor for a spore to form a visible colony also explains why $\sim$30% of *dcp2Δ* spores did not form visible colonies. Additionally, WGS of one of the nonevolved *dcp2Δ* strains revealed some reads corresponding to a *kap123* mutant allele, while other reads were from a wild-type *KAP123* allele (Figure S12A, nonevolved *dcp2Δ*_2). The presence of both alleles in the nonevolved *dcp2Δ* clearly indicates that this nonevolved population arose from a *KAP123 dcp2Δ* spore that obtained a *kap123* mutation during early growth. Thus, Dcp2 is likely not absolutely required for spore

germination and extremely slow growth, but in practical terms it is impossible to continuously culture *dcp2Δ* under laboratory conditions without suppressors. The question of whether *DCP2* should be categorized as an essential gene then becomes dependent on the definition of essential used.

Experimental evolution identifies novel bypass suppressors of dcp2Δ

Our experimental evolution approach to identifying suppressors in the decapping enzyme is distinct from previous genetics screens. All previous screens isolated suppressors of a partial defect in the decapping enzyme (*dcp2-7* or *dcp1-2*) and these suppressor mutations restored mRNA decapping by improving the function of the partially defective Dcp1/Dcp2 enzyme (Dunckley and Parker 1999; Dunckley *et al.* 2001; Kshirsagar and Parker 2004; Segal *et al.* 2006). Thus, these previous screens were helpful in identifying regulators of Dcp1/Dcp2, but they did not provide much insight into the importance of decapping for growth and cellular homeostasis. We designed our experimental evolution approach to complement these previous studies, reasoning that the use of a complete deletion of the *DCP2* gene would preclude selecting suppressors that restored Dcp1/Dcp2 function. Experimental evolution further allows for selection of suppressors with small effects on growth. Small effects on growth may not result in a readily observable effect on colony size in a traditional screen, but are selected slowly but surely in experimental evolution.

We identified nonsynonymous mutations in 16 different genes. Some of these mutations are likely to just have occurred randomly, and may not affect *dcp2Δ* growth. However, three genes were mutated multiple times and we concentrated our further analysis on those. We show that *kap123Δ*, *tl(gag)gΔ*, and *whi2Δ* loss-of-function mutations are each sufficient to suppress the growth defect of *dcp2Δ*. One advantage of experimental evolution is that multiple mutations can arise that act additively or even synergistically to further improve growth. This seems to have occurred since six of the eight isolates contain mutations in both *KAP123* and either *tL(GAG)G* or *WHI2*. Furthermore, we confirmed that the *dcp2Δ kap123Δ tl(gag)gΔ* triple mutant grew better than either the *dcp2Δ kap123Δ* or *dcp2Δ tl(gag)gΔ* double mutant. These observations indicate that the *kap123* and *tl(gag)g* mutations affect *dcp2* through different independent mechanisms.

Another advantage of experimental evolution is that it allows multiple mutations to arise where mutation of a particular gene can only improve growth after some other gene is mutated. We did not find clear evidence for this, although this might be the case for some of the mutations we only found once. Although we cannot completely trace the order in which each mutation arose, the comparison of duplicate evolved isolates derived from a common haploid spore indicates that some mutations arose early and others arose later (Figure S12A). This indicates that in lineage 4 a *tl(gag)g* mutation arose before a *kap123* mutation, while in lineage 2 the genes were mutated in the reverse order. The observation that *kap123* and *tl(gag)g* mutations can arise in both orders further confirms that they suppress *dcp2Δ* by independent mechanisms.

Although we have not formally proven it, several lines of evidence suggest that some of the 13 genes mutated only once also affect *dcp2Δ* growth. First, evolved isolate 2-1 contains a *kap123* mutation but wild-type *WHI2* and *tL(GAG)G* genes, yet grows just as well as some of the isolates with two suppressors. Thus, isolate 2-1 likely contains an additional suppressor. The only nonsynonymous mutation that differs between isolate 2-1 and the nonevolved parent is a single amino acid change in RNA polymerase II (*rpo21-R1281C*), and thus this may be a suppressor. Second, in lineage 3, both the *kap123* and *whi2* mutations arose late. This suggests that some other early mutation might have allowed us to recover the nonevolved starting strain. The only nonsynonymous mutation shared between isolates 3-1 and 3-2 is a frameshift in *CSE2*, which encodes a subunit of the mediator complex. Third, isolate 4-2 contains a mutation in the start codon for Psr1, which forms a complex with Whi2 (Kaida *et al.* 2002). Further analyses will be required to definitively determine whether these 13 other mutations also affect *dcp2Δ* growth.

The anticodon of an enigmatic tRNA affects growth of dcp2 strains

Although conservation in related species suggests *tL(GAG)G* is a functional gene, essentially nothing is known about its function. Previous studies have shown that deletion of *tL(GAG)G* did not affect growth and thus is not absolutely required for translation of CUC or CUU codons. However, *tl(gag)gΔ* showed synthetic phenotypes with the loss of *tL(UAG)* genes, suggesting some contribution to translation (Huang *et al.* 2012; Bloom-Ackermann *et al.* 2014). Furthermore, it was shown that mutating the anticodon of *tL(GAG)G* to UAG resulted in complementation of the lethality of a triple deletion of *tL(UAG)* genes, and thus this G34U mutant tRNA must be able to translate all 4 CUN codons (Huang *et al.* 2012). This G34U mutation that allows for translation of all four CUN codons is the same as the one that we show is sufficient to allow viability of *dcp2Δ*. Overall, previous research suggested that *tL(GAG)G* and *tL(UAG)* have overlapping functions, which does not explain why *tL(GAG)G* is conserved. Our results show that *tL(GAG)G* has a specific function that is not interchangeable with *tL(UAG)*.

It is interesting that no other components of the translation machinery were identified as *dcp2Δ* suppressors. In addition to *tL(GAG)G*, there are five other single-gene tRNAs. Four of them are essential, while *tR(CCU)J* is not. However, *tR(CCU)J* was not identified as *dcp2Δ* suppressor mutants. More broadly, none of the translation elongation factors, ribosomal subunits, or aminoacyl synthetases were mutated in our evolved strains. It is possible that these mutations would be found in a larger screen, but it seems unlikely that such a large number of genes would have been missed, while finding two alleles of the small *tL(GAG)G* gene. This makes it unlikely that a general translation elongation defect improves growth of *dcp2Δ*.

Because the anticodon sequence of *tL(GAG)G* affects growth of *dcp2*, but mutations affecting global translation elongation were not isolated, we propose that *tL(GAG)G* affects translation kinetics or accuracy of CUC or CUU codons, perhaps in some specific context. Further research will be required to determine whether translation at all CUC and CUU codons is affected by *tL(GAG)G* or whether a specific subset of these codons is affected, how this translation defect affects growth of *dcp2* strains, and whether this is related to the effect of codon optimality on mRNA degradation (Presnyak *et al.* 2015). Similarly, further research on Kap123 is required to fully understand how it affects *dcp2Δ* growth. Although Kap123 is a karyopherin and has been shown to physically interact with dozens of proteins, its function is largely redundant with other karyopherins, including kap121 (Aitchison and Rout 2012). The only nuclear protein that is known to be mislocalized in *kap123Δ* is the ribosome biogenesis protein Ecm1 (Yao *et al.* 2010). In addition, the normally cytoplasmic proteins Srp68 (Grosshans *et al.* 2001) and Aim44 (Perez and Thorner 2019) become localized to the nucleus if overexpressed, which requires Kap123. The identity of the Kap123 client that affects *dcp2Δ* growth therefore remains to be determined.

Bypass suppressors of dcp2Δ do not restore mRNA decay rate or direction to normal

Previous genetic screens of suppressors of *dcp1* or *dcp2* defects have identified "enhancer of decapping" genes that restored decapping to a partially defective Dcp1-Dcp2 complex (Dunckley and Parker 1999; Dunckley *et al.* 2001; Kshirsagar and Parker 2004; Segal *et al.* 2006). We expected to either isolate mutations that activate alternative mRNA degradation pathways or mutations that allow survival despite slow mRNA decay. Follow-up experiments indicate that we isolated the latter. We observed that the suppressor mutations isolated here do not appear to restore the 5′ to 3′ decay of mRNA, nor the overall rate of mRNA degradation to wild-type levels. These analyses on select model mRNAs cannot rule out either small effects, or effects on a subset of mRNAs, but we favor the simpler explanation that the suppressor mutations improve growth while maintaining the relatively slow RNA exosome-mediated 3′ to 5′ decay of mRNA.

Bypass suppressors of dcp2Δ do not have a major effect on the transcriptome

Finally, we studied the effect of *kap123Δ* and *tl(gag)gΔ* on the transcriptome. Limitations of this study include that we had to use a *dcp2-7* strain because *dcp2Δ* strains could not be cultured without suppressors arising, and thus could not be used as a single mutant control to compare to the double mutants. Although *dcp2-7* causes a decapping defect at the restrictive temperature, this defect is not complete. Comparing *dcp2-7* to wild type, we observed global disruption in transcriptome homeostasis, confirming previous publications (Geisler *et al.* 2012; He and Jacobson 2015; Celik *et al.* 2017). We suspect that the detected changes are dominated by indirect effects and thus cannot be used to identify which transcripts are differentially decapped. Strikingly, GO analysis indicated a significant enrichment of snoRNA loci among the transcripts that were differentially expressed between *dcp2-7* and *dcp2-7 kap123Δ tl(gag)gΔ* (Figure S10B). snoRNA processing pathways are well established and do not involve decapping of snoRNA transcripts. In fact, some mature snoRNAs retain the cap structure while, for other snoRNAs, the Rnt1 endonuclease removes the cap. Both of these classes of snoRNAs were affected. For example, the snR9 snoRNA is well established to retain its cap (Wise *et al.* 1983) and is not processed by Rnt1 (Chanfreau *et al.* 1998a), while both snR190 and snR128 are 5′ processed by Rnt1 (Chanfreau *et al.* 1998b), yet all three are similarly affected by Dcp2 inactivation (Figure 9, B and C). Thus, Dcp2 inactivation appears to indirectly affect transcripts from the snoRNA loci, and the *kap123Δ* and *tl(gag)gΔ* suppressors partially suppress this defect. Although this analysis cannot determine whether the partially restored snoRNA misregulation is a cause or an effect of improved growth, the fact that we did not find mutations in either snoRNA genes or genes involved in the snoRNA biogenesis from our WGS analysis suggests that snoRNA expression effects are a consequence of improved growth. Although snoRNAs were enriched among transcripts whose partial restoration upon *kap123Δ tl(gag)gΔ* reaches statistical significance, we observed by linear regression that mRNAs and XUTs follow a similar trend, but perhaps are not as sensitive to *kap123Δ tl(gag)gΔ*. Although many genes showed a smaller change in the suppressor strains, the effect was small, which likely explains why DESeq2 could not identify any specific genes for which the data reached statistical significance. Our findings that suppressor mutations (partially) alleviate the effect of decapping defects, and that most previous transcriptome-wide studies inadvertently used strains with suppressors imply that most previous studies likely underestimated the transcriptome-wide effects of decapping defects.

Implications

Our results suggest that studies on decapping mutants should be carefully controlled for unanticipated suppressors. Depending on the goals, it might be preferred to compare a *dcp2Δ kap123Δ tl(gag)gΔ* strain to a *kap123Δ tl(gag)gΔ* control, thereby reducing the selection for inadvertent suppressors. Finally, the observation that suppressors can readily occur during growth under standard laboratory conditions, and especially during extended culture is not surprising, and is unlikely to be specific for either *dcp2* mutations or for *S. cerevisiae*. We therefore suggest that unexpected phenotypes, or conflicting phenotypes, should be resolved by WGS in organisms such as yeast, where this is feasible for a reasonable cost.

Acknowledgments

This work was supported by National Institutes of Health grant R01-GM099790 to A.v.H. We thank members of the

van Hoof laboratory for critical discussions, Kate Travis for performing pilot experiments for the experimental evolution, Lee-Ann Notice for help with analyzing tRNA mutations, and Jaeil Han for insightful comments throughout. Antibodies to Kap123 were a kind gift from Valerie Doye (Institut Jaque Monod) and initially developed by Michael Rexach (University of California, Santa Cruz). The yRP1346 *dcp2Δ* strain was a kind gift from Roy Parker (University of Colorado). We thank William Margolin (University of Texas Health Science Center at Houston) for microscope usage; Kevin Morano (University of Texas Health Science Center at Houston) for microplate reader usage; and Cesar Arias, Diana Panesso, and An Dihn (University of Texas Health Science Center at Houston) for whole-genome sequencing of the *DCP2/dcp2Δ* starting diploid strain.

Literature Cited

Aitchison, J. D., and M. P. Rout, 2012 The yeast nuclear pore complex and transport through it. Genetics 190: 855–883. https://doi.org/10.1534/genetics.111.127803

Anderson, J. S., and R. Parker, 1998 The 3′ to 5′ degradation of yeast mRNAs is a general mechanism for mRNA turnover that requires the SKI2 DEVH box protein and 3′ to 5′ exonucleases of the exosome complex. EMBO J. 17: 1497–1506. https://doi.org/10.1093/emboj/17.5.1497

Beelman, C. A., A. Stevens, G. Caponigro, T. E. LaGrandeur, L. Hatfield *et al*., 1996 An essential component of the decapping enzyme required for normal rates of mRNA turnover. Nature 382: 642–646. https://doi.org/10.1038/382642a0

Blanc, A., J. C. Ribas, R. B. Wickner, and N. Sonenberg, 1994 His-154 is involved in the linkage of the Saccharomyces cerevisiae L-A double-stranded RNA virus Gag protein to the cap structure of mRNAs and is essential for M1 satellite virus expression. Mol. Cell. Biol. 14: 2664–2674. https://doi.org/10.1128/MCB.14.4.2664

Bloom-Ackermann, Z., S. Navon, H. Gingold, R. Towers, Y. Pilpel *et al*., 2014 A comprehensive tRNA deletion library unravels the genetic architecture of the tRNA pool. PLoS Genet. 10: e1004084. https://doi.org/10.1371/journal.pgen.1004084

Celik, A., R. Baker, F. He, and A. Jacobson, 2017 High-resolution profiling of NMD targets in yeast reveals translational fidelity as a basis for substrate selection. RNA 23: 735–748. https://doi.org/10.1261/rna.060541.116

Chanfreau, G., P. Legrain, and A. Jacquier, 1998a Yeast RNase III as a key processing enzyme in small nucleolar RNAs metabolism. J. Mol. Biol. 284: 975–988. https://doi.org/10.1006/jmbi.1998.2237

Chanfreau, G., G. Rotondo, P. Legrain, and A. Jacquier, 1998b Processing of a dicistronic small nucleolar RNA precursor by the RNA endonuclease Rnt1. EMBO J. 17: 3726–3737. https://doi.org/10.1093/emboj/17.13.3726

Chang, J. H., X. Jiao, K. Chiba, C. Oh, C. E. Martin *et al*., 2012 Dxo1 is a new type of eukaryotic enzyme with both decapping and 5′-3′ exoribonuclease activity. Nat. Struct. Mol. Biol. 19: 1011–1017. https://doi.org/10.1038/nsmb.2381

Chen, X., G. Wang, Y. Zhang, M. Dayhoff-Brannigan, N. L. Diny *et al*., 2018 Whi2 is a conserved negative regulator of TORC1 in response to low amino acids. PLoS Genet. 14: e1007592. https://doi.org/10.1371/journal.pgen.1007592

Cherry, P. D., S. E. Peach, and J. R. Hesselberth, 2019 Multiple decay events target HAC1 mRNA during splicing to regulate the unfolded protein response. eLife 8: e42262. https://doi.org/10.7554/eLife.42262

Chook, Y. M., and K. E. Suel, 2011 Nuclear import by karyopherin-βs: recognition and inhibition. Biochim. Biophys. Acta 1813: 1593–1606. https://doi.org/10.1016/j.bbamcr.2010.10.014

Cingolani, P., V. M. Patel, M. Coon, T. Nguyen, S. J. Land *et al*., 2012 Using Drosophila melanogaster as a model for genotoxic chemical mutational studies with a new program, SnpSift. Front. Genet. 3: 35. https://doi.org/10.3389/fgene.2012.00035

Comyn, S. A., S. Flibotte, and T. Mayor, 2017 Recurrent background mutations in WHI2 impair proteostasis and degradation of misfolded cytosolic proteins in Saccharomyces cerevisiae. Sci. Rep. 7: 4183. https://doi.org/10.1038/s41598-017-04525-8

Doamekpor, S. K., A. Gozdek, A. Kwasnik, J. Kufel, and L. Tong, 2020 A novel 5′-hydroxyl dinucleotide hydrolase activity for the DXO/Rai1 family of enzymes. Nucleic Acids Res. 48: 349–358. https://doi.org/10.1093/nar/gkz1107

Doma, M. K., and R. Parker, 2006 Endonucleolytic cleavage of eukaryotic mRNAs with stalls in translation elongation. Nature 440: 561–564. https://doi.org/10.1038/nature04530

Dunckley, T., and R. Parker, 1999 The DCP2 protein is required for mRNA decapping in Saccharomyces cerevisiae and contains a functional MutT motif. EMBO J. 18: 5411–5422. https://doi.org/10.1093/emboj/18.19.5411

Dunckley, T., M. Tucker, and R. Parker, 2001 Two related proteins, Edc1p and Edc2p, stimulate mRNA decapping in Saccharomyces cerevisiae. Genetics 157: 27–37.

D'Orazio, K. N., C. C. Wu, N. Sinha, R. Loll-Krippleber, G. W. Brown *et al*., 2019 The endonuclease Cue2 cleaves mRNAs at stalled ribosomes during no go decay. eLife 8: e49117. https://doi.org/10.7554/eLife.49117

Floch, A. G., D. Tareste, P. F. Fuchs, A. Chadrin, I. Naciri *et al*., 2015 Nuclear pore targeting of the yeast Pom33 nucleoporin depends on karyopherin and lipid binding. J. Cell Sci. 128: 305–316. https://doi.org/10.1242/jcs.158915

Fujimura, T., and R. Esteban, 2011 Cap-snatching mechanism in yeast L-A double-stranded RNA virus. Proc. Natl. Acad. Sci. USA 108: 17667–17671. https://doi.org/10.1073/pnas.1111900108

Fujimura, T., and R. Esteban, 2012 Cap snatching of yeast L-A double-stranded RNA virus can operate in trans and requires viral polymerase actively engaging in transcription. J. Biol. Chem. 287: 12797–12804. https://doi.org/10.1074/jbc.M111.327676

Geisler, S., L. Lojek, A. M. Khalil, K. E. Baker, and J. Coller, 2012 Decapping of long noncoding RNAs regulates inducible genes. Mol. Cell 45: 279–291. https://doi.org/10.1016/j.molcel.2011.11.025

Giaever, G., A. M. Chu, L. Ni, C. Connelly, L. Riles *et al*., 2002 Functional profiling of the Saccharomyces cerevisiae genome. Nature 418: 387–391. https://doi.org/10.1038/nature00935

Grosshans, H., K. Deinert, E. Hurt, and G. Simos, 2001 Biogenesis of the signal recognition particle (SRP) involves import of SRP proteins into the nucleolus, assembly with the SRP-RNA, and Xpo1p- mediated export. J. Cell Biol. 153: 745–762. https://doi.org/10.1083/jcb.153.4.745

Grudzien-Nogalska, E., X. Jiao, M. G. Song, R. P. Hart, and M. Kiledjian, 2016 Nudt3 is an mRNA decapping enzyme that modulates cell migration. RNA 22: 773–781. https://doi.org/10.1261/rna.055699.115

He, F., and A. Jacobson, 2015 Control of mRNA decapping by positive and negative regulatory elements in the Dcp2 C-terminal domain. RNA 21: 1633–1647. https://doi.org/10.1261/rna.052449.115

He, F., X. Li, P. Spatrick, R. Casillo, S. Dong *et al*., 2003 Genome-wide analysis of mRNAs regulated by the nonsense-mediated and 5′ to 3′ mRNA decay pathways in yeast. Mol. Cell 12: 1439–1452. https://doi.org/10.1016/S1097-2765(03)00446-5

He, F., N. Amrani, M. J. Johansson, and A. Jacobson, 2008 Chapter 6. Qualitative and quantitative assessment of the activity of

the yeast nonsense-mediated mRNA decay pathway. Methods Enzymol. 449: 127–147. https://doi.org/10.1016/S0076-6879(08)02406-3

He, F., C. Li, B. Roy, and A. Jacobson, 2014 Yeast Edc3 targets RPS28B mRNA for decapping by binding to a 3′ untranslated region decay-inducing regulatory element. Mol. Cell. Biol. 34: 1438–1451. https://doi.org/10.1128/MCB.01584-13

He, F., A. Celik, C. Wu, and A. Jacobson, 2018 General decapping activators target different subsets of inefficiently translated mRNAs. eLife 7: e34409. https://doi.org/10.7554/eLife.34409

Huang, Q., P. Yao, G. Eriani, and E. D. Wang, 2012 In vivo identification of essential nucleotides in tRNALeu to its functions by using a constructed yeast tRNALeu knockout strain. Nucleic Acids Res. 40: 10463–10477. https://doi.org/10.1093/nar/gks783

Jiao, X., S. Xiang, C. Oh, C. E. Martin, L. Tong *et al.*, 2010 Identification of a quality-control mechanism for mRNA 5′-end capping. Nature 467: 608–611. https://doi.org/10.1038/nature09338

Jinek, M., S. M. Coyle, and J. A. Doudna, 2011 Coupled 5′ nucleotide recognition and processivity in Xrn1-mediated mRNA decay. Mol. Cell 41: 600–608. https://doi.org/10.1016/j.molcel.2011.02.004

Jungfleisch, J., D. D. Nedialkova, I. Dotu, K. E. Sloan, N. Martinez-Bosch *et al.*, 2017 A novel translational control mechanism involving RNA structures within coding sequences. Genome Res. 27: 95–106 (erratum: Genome Res. 27: 663). https://doi.org/10.1101/gr.209015.116

Kaida, D., H. Yashiroda, A. Toh-e, and Y. Kikuchi, 2002 Yeast Whi2 and Psr1-phosphatase form a complex and regulate STRE-mediated gene expression. Genes Cells 7: 543–552. https://doi.org/10.1046/j.1365-2443.2002.00538.x

Kim, D., G. Pertea, C. Trapnell, H. Pimentel, R. Kelley *et al.*, 2013 TopHat2: accurate alignment of transcriptomes in the presence of insertions, deletions and gene fusions. Genome Biol. 14: R36. https://doi.org/10.1186/gb-2013-14-4-r36

Kshirsagar, M., and R. Parker, 2004 Identification of Edc3p as an enhancer of mRNA decapping in Saccharomyces cerevisiae. Genetics 166: 729–739. https://doi.org/10.1534/genetics.166.2.729

Langmead, B., C. Trapnell, M. Pop, and S. L. Salzberg, 2009 Ultrafast and memory-efficient alignment of short DNA sequences to the human genome. Genome Biol. 10: R25. https://doi.org/10.1186/gb-2009-10-3-r25

Lang, G. I., D. P. Rice, M. J. Hickman, E. Sodergren, G. M. Weinstock *et al.*, 2013 Pervasive genetic hitchhiking and clonal interference in forty evolving yeast populations. Nature 500: 571–574. https://doi.org/10.1038/nature12344

Larimer, F. W., C. L. Hsu, M. K. Maupin, and A. Stevens, 1992 Characterization of the XRN1 gene encoding a 5′→3′ exoribonuclease: sequence data and analysis of disparate protein and mRNA levels of gene-disrupted yeast cells. Gene 120: 51–57. https://doi.org/10.1016/0378-1119(92)90008-D

Lee, C. Y., A. Lee, and G. Chanfreau, 2003 The roles of endonucleolytic cleavage and exonucleolytic digestion in the 5′-end processing of S. cerevisiae box C/D snoRNAs. RNA 9: 1362–1370. https://doi.org/10.1261/rna.5126203

Liao, Y., G. K. Smyth, and W. Shi, 2014 featureCounts: an efficient general purpose program for assigning sequence reads to genomic features. Bioinformatics 30: 923–930. https://doi.org/10.1093/bioinformatics/btt656

Li, Y., M. Song, and M. Kiledjian, 2011 Differential utilization of decapping enzymes in mammalian mRNA decay pathways. RNA 17: 419–428. https://doi.org/10.1261/rna.2439811

Liu, H., N. D. Rodgers, X. Jiao, and M. Kiledjian, 2002 The scavenger mRNA decapping enzyme DcpS is a member of the HIT family of pyrophosphatases. EMBO J. 21: 4699–4708. https://doi.org/10.1093/emboj/cdf448

Liu, G., M. Y. Yong, M. Yurieva, K. G. Srinivasan, J. Liu *et al.*, 2015 Gene essentiality is a quantitative property linked to cellular evolvability. Cell 163: 1388–1399. https://doi.org/10.1016/j.cell.2015.10.069

Love, M. I., W. Huber, and S. Anders, 2014 Moderated estimation of fold change and dispersion for RNA-seq data with DESeq2. Genome Biol. 15: 550. https://doi.org/10.1186/s13059-014-0550-8

Makanae, K., R. Kintaka, T. Makino, H. Kitano, and H. Moriya, 2013 Identification of dosage-sensitive genes in Saccharomyces cerevisiae using the genetic tug-of-war method. Genome Res. 23: 300–311. https://doi.org/10.1101/gr.146662.112

Mouaikel, J., C. Verheggen, E. Bertrand, J. Tazi, and R. Bordonne, 2002 Hypermethylation of the cap structure of both yeast snRNAs and snoRNAs requires a conserved methyltransferase that is localized to the nucleolus. Mol. Cell 9: 891–901. https://doi.org/10.1016/S1097-2765(02)00484-7

Muhlrad, D., C. J. Decker, and R. Parker, 1994 Deadenylation of the unstable mRNA encoded by the yeast MFA2 gene leads to decapping followed by 5′→3′ digestion of the transcript. Genes Dev. 8: 855–866. https://doi.org/10.1101/gad.8.7.855

Ooi, S. L., D. A. Samarsky, M. J. Fournier, and J. D. Boeke, 1998 Intronic snoRNA biosynthesis in Saccharomyces cerevisiae depends on the lariat-debranching enzyme: intron length effects and activity of a precursor snoRNA. RNA 4: 1096–1110. https://doi.org/10.1017/S1355838298980785

Parker, R., 2012 RNA degradation in Saccharomyces cerevisae. Genetics 191: 671–702. https://doi.org/10.1534/genetics.111.137265

Patel, S. S., and M. F. Rexach, 2008 Discovering novel interactions at the nuclear pore complex using bead halo: a rapid method for detecting molecular interactions of high and low affinity at equilibrium. Mol. Cell. Proteomics 7: 121–131. https://doi.org/10.1074/mcp.M700407-MCP200

Perez, A. M., and J. Thorner, 2019 Septin-associated proteins Aim44 and Nis1 traffic between the bud neck and the nucleus in the yeast Saccharomyces cerevisiae. Cytoskeleton (Hoboken) 76: 15–32. https://doi.org/10.1002/cm.21500

Presnyak, V., N. Alhusaini, Y. H. Chen, S. Martin, N. Morris *et al.*, 2015 Codon optimality is a major determinant of mRNA stability. Cell 160: 1111–1124. https://doi.org/10.1016/j.cell.2015.02.029

Qu, L. H., A. Henras, Y. J. Lu, H. Zhou, W. X. Zhou *et al.*, 1999 Seven novel methylation guide small nucleolar RNAs are processed from a common polycistronic transcript by Rat1p and RNase III in yeast. Mol. Cell. Biol. 19: 1144–1158. https://doi.org/10.1128/MCB.19.2.1144

Radhakrishnan, A., Y. H. Chen, S. Martin, N. Alhusaini, R. Green *et al.*, 2016 The DEAD-Box protein Dhh1p couples mRNA decay and translation by monitoring codon optimality. Cell 167: 122–132.e9. https://doi.org/10.1016/j.cell.2016.08.053

Rockmill, B., E. J. Lambie, and G. S. Roeder, 1991 Spore enrichment. Methods Enzymol. 194: 146–149. https://doi.org/10.1016/0076-6879(91)94012-2

Santos, M. A., V. M. Perreau, and M. F. Tuite, 1996 Transfer RNA structural change is a key element in the reassignment of the CUG codon in Candida albicans. EMBO J. 15: 5060–5068. https://doi.org/10.1002/j.1460-2075.1996.tb00886.x

Schaeffer, D., S. Meaux, A. Clark, and A. van Hoof, 2008 Determining in vivo activity of the yeast cytoplasmic exosome. Methods Enzymol. 448: 227–239. https://doi.org/10.1016/S0076-6879(08)02612-8

Segal, S. P., T. Dunckley, and R. Parker, 2006 Sbp1p affects translational repression and decapping in Saccharomyces cerevisiae. Mol. Cell. Biol. 26: 5120–5130 [corrigenda: Mol. Cell. Biol. 27: 789–790 (2007)]. https://doi.org/10.1128/MCB.01913-05

Sidrauski, C., and P. Walter, 1997 The transmembrane kinase Ire1p is a site-specific endonuclease that initiates mRNA splicing in the unfolded protein response. Cell 90: 1031–1039. https://doi.org/10.1016/S0092-8674(00)80369-4

Silva, R. M., J. A. Paredes, G. R. Moura, B. Manadas, T. Lima-Costa *et al.*, 2007 Critical roles for a genetic code alteration in the evolution of the genus Candida. EMBO J. 26: 4555–4565. https://doi.org/10.1038/sj.emboj.7601876

Song, M. G., Y. Li, and M. Kiledjian, 2010 Multiple mRNA decapping enzymes in mammalian cells. Mol. Cell 40: 423–432. https://doi.org/10.1016/j.molcel.2010.10.010

Stevens, A., and T. L. Poole, 1995 5′-exonuclease-2 of Saccharomyces cerevisiae. Purification and features of ribonuclease activity with comparison to 5′-exonuclease-1. J. Biol. Chem. 270: 16063–16069. https://doi.org/10.1074/jbc.270.27.16063

Teng, X., M. Dayhoff-Brannigan, W. C. Cheng, C. E. Gilbert, C. N. Sing *et al.*, 2013 Genome-wide consequences of deleting any single gene. Mol. Cell 52: 485–494. https://doi.org/10.1016/j.molcel.2013.09.026

Tsuboi, T., R. Yamazaki, R. Nobuta, K. Ikeuchi, S. Makino *et al.*, 2015 The tRNA splicing endonuclease complex cleaves the mitochondria-localized CBP1 mRNA. J. Biol. Chem. 290: 16021–16030. https://doi.org/10.1074/jbc.M114.634592

van Dijk, E. L., C. L. Chen, Y. d'Aubenton-Carafa, S. Gourvennec, M. Kwapisz *et al.*, 2011 XUTs are a class of Xrn1-sensitive antisense regulatory non-coding RNA in yeast. Nature 475: 114–117. https://doi.org/10.1038/nature10118

van Hoof, A., R. R. Staples, R. E. Baker, and R. Parker, 2000 Function of the ski4p (Csl4p) and Ski7p proteins in 3′-to-5′ degradation of mRNA. Mol. Cell. Biol. 20: 8230–8243. https://doi.org/10.1128/MCB.20.21.8230-8243.2000

Webster, M. W., Y. H. Chen, J. A. W. Stowell, N. Alhusaini, T. Sweet *et al.*, 2018 mRNA deadenylation is coupled to translation rates by the differential activities of Ccr4-Not nucleases. Mol Cell 70: 1089–1100.e8. https://doi.org/10.1016/j.molcel.2018.05.033

Wery, M., M. Descrimes, N. Vogt, A. S. Dallongeville, D. Gautheret *et al.*, 2016 Nonsense-mediated decay restricts LncRNA levels in yeast unless blocked by double-stranded RNA structure. Mol. Cell 61: 379–392. https://doi.org/10.1016/j.molcel.2015.12.020

Wise, J. A., D. Tollervey, D. Maloney, H. Swerdlow, E. J. Dunn *et al.*, 1983 Yeast contains small nuclear RNAs encoded by single copy genes. Cell 35: 743–751. https://doi.org/10.1016/0092-8674(83)90107-1

Xiang, S., A. Cooper-Morgan, X. Jiao, M. Kiledjian, J. L. Manley *et al.*, 2009 Structure and function of the 5′→3′ exoribonuclease Rat1 and its activating partner Rai1. Nature 458: 784–788. https://doi.org/10.1038/nature07731

Yao, Y., E. Demoinet, C. Saveanu, P. Lenormand, A. Jacquier *et al.*, 2010 Ecm1 is a new pre-ribosomal factor involved in pre-60S particle export. RNA 16: 1007–1017. https://doi.org/10.1261/rna.2012310

Zeidan, Q., F. He, F. Zhang, H. Zhang, A. Jacobson *et al.*, 2018 Conserved mRNA-granule component Scd6 targets Dhh1 to repress translation initiation and activates Dcp2-mediated mRNA decay in vivo. PLoS Genet. 14: e1007806 [corrigenda: PLoS Genet. 15: e1008299 (2019)]. https://doi.org/10.1371/journal.pgen.1007806

Zhou, M., S. Bail, H. L. Plasterer, J. Rusche, and M. Kiledjian, 2015 DcpS is a transcript-specific modulator of RNA in mammalian cells. RNA 21: 1306–1312. https://doi.org/10.1261/rna.051573.115

Zhu, Y. O., M. L. Siegal, D. W. Hall, and D. A. Petrov, 2014 Precise estimates of mutation rate and spectrum in yeast. Proc. Natl. Acad. Sci. USA 111: E2310–E2318. https://doi.org/10.1073/pnas.1323011111

Communicating editor: E. Tran